

---

# The Heliospheric Magnetic Field

Mathew J. Owens

Department of Meteorology  
University of Reading  
Earley Gate  
Reading RG6 6BB  
United Kingdom

email: [m.j.owens@reading.ac.uk](mailto:m.j.owens@reading.ac.uk)

<http://www.met.reading.ac.uk/~vy902033>

Robert J. Forsyth

The Blackett Laboratory  
Imperial College London  
Prince Consort Road  
London SW7 2AZ  
United Kingdom

email: [r.forsyth@imperial.ac.uk](mailto:r.forsyth@imperial.ac.uk)

Accepted: 10 November 2013

Published: 28 November 2013

## Abstract

The heliospheric magnetic field (HMF) is the extension of the coronal magnetic field carried out into the solar system by the solar wind. It is the means by which the Sun interacts with planetary magnetospheres and channels charged particles propagating through the heliosphere. As the HMF remains rooted at the solar photosphere as the Sun rotates, the large-scale HMF traces out an Archimedean spiral. This pattern is distorted by the interaction of fast and slow solar wind streams, as well as the interplanetary manifestations of transient solar eruptions called coronal mass ejections. On the smaller scale, the HMF exhibits an array of waves, discontinuities, and turbulence, which give hints to the solar wind formation process. This review aims to summarise observations and theory of the small- and large-scale structure of the HMF. Solar-cycle and cycle-to-cycle evolution of the HMF is discussed in terms of recent spacecraft observations and pre-spaceage proxies for the HMF in geomagnetic and galactic cosmic ray records.

**Keywords:** Heliosphere, Magnetic field, Solar wind

## Imprint / Terms of Use

*Living Reviews in Solar Physics* is a peer reviewed open access journal published by the Max Planck Institute for Solar System Research, Max-Planck-Str. 2, 37191 Katlenburg-Lindau, Germany. ISSN 1614-4961.

This review is licensed under a Creative Commons Attribution-Non-Commercial 3.0 Germany License: <http://creativecommons.org/licenses/by-nc/3.0/de/>. Figures that have been previously published elsewhere may not be reproduced without consent of the original copyright holders.

Because a *Living Reviews* article can evolve over time, we recommend to cite the article as follows:

Mathew J. Owens and Robert J. Forsyth,  
“The Heliospheric Magnetic Field”,  
*Living Rev. Solar Phys.*, **10**, (2013), 5. URL (accessed <date>):  
<http://www.livingreviews.org/lrsp-2013-5>

The date given as <date> then uniquely identifies the version of the article you are referring to.

## Article Revisions

*Living Reviews* supports two ways of keeping its articles up-to-date:

**Fast-track revision.** A fast-track revision provides the author with the opportunity to add short notices of current research results, trends and developments, or important publications to the article. A fast-track revision is refereed by the responsible subject editor. If an article has undergone a fast-track revision, a summary of changes will be listed here.

**Major update.** A major update will include substantial changes and additions and is subject to full external refereeing. It is published with a new publication number.

For detailed documentation of an article’s evolution, please refer to the history document of the article’s online version at <http://www.livingreviews.org/lrsp-2013-5>.

# Contents

<b>1</b>	<b>Introduction</b>	<b>5</b>
<b>2</b>	<b>Steady State Heliosphere</b>	<b>6</b>
2.1	Magnetic origin of the solar wind . . . . .	6
2.2	Photospheric extrapolations . . . . .	6
2.3	Parker spiral magnetic field . . . . .	7
2.4	Solar minimum: Quasi-dipolar magnetic field . . . . .	11
2.5	Stream interaction regions . . . . .	14
2.6	Outer heliosphere . . . . .	17
<b>3</b>	<b>Particle Probes of the HMF</b>	<b>19</b>
3.1	Suprathermal electrons . . . . .	19
3.2	High-energy particles . . . . .	20
<b>4</b>	<b>Transient and Fine-scale Structure</b>	<b>22</b>
4.1	Deviations from the Parker model . . . . .	22
4.2	Interplanetary coronal mass ejections . . . . .	23
4.2.1	Magnetic clouds . . . . .	23
4.2.2	Relation of CMEs to the HMF . . . . .	25
4.3	Fine-scale structure . . . . .	25
<b>5</b>	<b>Solar Cycle Variations</b>	<b>28</b>
5.1	Solar minimum and the rise/declining phases . . . . .	28
5.2	Solar maximum . . . . .	29
5.3	The space age solar cycles . . . . .	29
5.4	Models of solar-cycle evolution . . . . .	31
5.5	Long-term evolution of the HMF . . . . .	33
5.5.1	Geomagnetic activity . . . . .	33
5.5.2	Sunspot records . . . . .	33
5.5.3	Cosmogenic isotope records . . . . .	33
<b>6</b>	<b>Summary</b>	<b>35</b>
	<b>References</b>	<b>37</b>



## 1 Introduction

The solar corona is a highly conductive, magnetically-dominated plasma. With increasing height through the solar corona, increasing temperature results in pressure-driven solar wind outflow (Parker, 1958) and within a few solar radii, the flow momentum is comparable to the magnetic pressure. Thus, the solar wind drags the coronal magnetic field out into the solar system, forming the heliospheric magnetic field (HMF), historically referred to as the interplanetary magnetic field (IMF), which pervades the entire heliosphere. The structure and dynamics of the HMF are key to understanding and forecasting space weather, as it directly couples the Sun with planetary magnetospheres, as well as channeling the flow of solar and cosmic energetic particles. The HMF is also the only aspect of the solar magnetic field which is accessible to direct measurement, providing strong constraints on theories of solar wind formation and the solar dynamo.

Information about the HMF can be obtained through a variety of indirect means, as discussed in Sections 2.2 and 3, but the bulk of our understanding comes from spacecraft-borne magnetometers, which make in situ observations of the of HMF. The first observations of the near-Earth solar wind were made by the Mariner spacecraft in the early 1960s. Subsequent spacecraft in near-Earth space have provided a reasonably complete record of the near-Earth heliospheric magnetic field since 1965. The OMNI dataset (see Section 5.3) collates the near-Earth solar wind measurements from numerous spacecraft. A full review of all heliospheric spacecraft is beyond the scope of this review, but there are a number which bear particular note as they form the basis of much of the discussion in the rest of the paper. Pioneer 10 and 11 (Smith *et al.*, 1975), launched in the early 1970s, were the first spacecraft to explore beyond 1 AU. While contact has been lost, Pioneer 10 was tracked to nearly 80 AU. Voyager 1 and 2 (Behannon *et al.*, 1977) were launched in 1977. Both have scientific instruments still operating. Voyager 1 crossed the termination shock in 2004 at 94.5 AU and recently became the first spacecraft to cross the heliopause at 121.6 AU and enter interstellar space. Voyager 2, following behind, crossed the termination shock at 84 AU in 2007. See Section 2.6 for further detail. Helios 1 and 2 (Searce *et al.*, 1975), launched in 1974 and 1976, explored the inner heliosphere in the ecliptic plane between 0.3 and 1 AU from the Sun. Ulysses (Balogh *et al.*, 1992), launched in 1990 into an approximately 6-year orbit of the Sun inclined at 80.2° to the solar equator, with perihelion at 1.3 AU and aphelion at 5.4 AU. It was the first spacecraft to explore the 3-dimensional structure of the heliosphere over a large latitude range. Operations ceased in 2009 after nearly 3 orbits. Finally, STEREO (Acuña *et al.*, 2008), launched in 2006, consists of two spacecraft at 1 AU separating in solar longitude ahead of and behind the Earth. They carry instrumentation aimed at obtaining stereoscopic views of the Sun and making multi-point in-situ measurements of the solar wind and HMF.

There have been a number of excellent reviews of the HMF (e.g., Balogh and Erdős, 2013; Zurbuchen, 2007), particularly focussed on the three-dimensional structure revealed by the Ulysses spacecraft (Smith, 2008). Here, we hope to incorporate observations from the most recent solar cycle and put it in context of the long-term evolution of the HMF. Recent models of HMF evolution will also be discussed. Section 2 introduces the steady-state heliosphere, an approximation most valid when the solar corona is slowly evolving over a solar rotation period, such as times close to solar minimum. Section 3 briefly discusses particle probes of the HMF, as these underpin our understanding of transient HMF structures summarised in Section 4. Section 5 discusses the evolution of the HMF over the solar cycle, including the long-term variation of the HMF inferred from proxy data.

## 2 Steady State Heliosphere

The solar magnetic field evolves on a range of time scales, from seconds to centuries. At the shortest time scales, waves and turbulence result in fine-scale HMF structure, briefly reviewed in Section 4.3. The solar wind, and hence the HMF, exhibits recurrence at the  $\sim 25.4$ -day solar rotation period, explained in Sections 2.4 and 2.5. Evolution on the scale of the 11-year solar cycle is discussed in Section 5 and the century scale variations evident from geomagnetic records specifically in Section 5.5. Nevertheless, much of the structure of the HMF can be understood by the steady-state approximation.

### 2.1 Magnetic origin of the solar wind

The solar corona is a low beta, high conductivity plasma. Thus, coronal dynamics are dominated by the evolution of the coronal magnetic field, which in turn is driven by plasma motions in the photosphere. The coronal plasma is heated to around 1–2 million Kelvin, by processes which are still under debate (e.g., Cranmer, 2008; McComas *et al.*, 2007), though it must involve the coronal magnetic field as it is the only source of sufficient energy density. The high coronal temperature leads to the formation of the solar wind, which becomes super-Alfvénic within 10–20 solar radii. The solar wind drags the coronal magnetic field out into the heliosphere, forming the HMF. Thus, the large scale structure and dynamics of the HMF is governed by the solar wind flow, which in turn has its origin in the magnetic structure of the corona. The simplest steady-state picture is observed under solar minimum conditions when the coronal magnetic field is closest to dipolar, typically with the magnetic dipole axis tilted by a few degrees to the solar rotation axis. The corona is observed to be organised into a belt of dense bright streamers around the magnetic equator with darker polar coronal holes in the high latitude regions. At this time fast solar wind (typical speeds  $\sim 750 \text{ km s}^{-1}$ ) fills most of the heliosphere, flowing outwards from the Sun from the regions of open magnetic field lines originating in the polar coronal holes. However, a belt of slower solar wind (typical speeds  $\sim 300\text{--}400 \text{ km s}^{-1}$ ) of about  $20^\circ$  latitudinal width originates from the streamer belt region corresponding to the magnetic equator. The magnetic field boundary separating oppositely directed magnetic field lines originating from the northern and southern polar coronal holes is carried out by this slower solar wind to form the heliospheric current sheet (HCS), a large scale magnetic boundary which extends throughout the heliosphere. The heliospheric magnetic field structure which arises under these conditions is described in more detail in Sections 2.3 and 2.4 and the evolution into a more complex field structure under solar maximum conditions in Section 5.2.

### 2.2 Photospheric extrapolations

Remote observations of the photospheric magnetic field have the potential to give us a valuable synoptic picture of the coronal magnetic field which is vital in understanding the global structure of the HMF. The line-of-sight component of the photospheric magnetic field can be routinely imaged using ground- and space-based magnetographs (e.g., Hoeksema and Scherrer, 1986). Most of this photospheric flux is “closed” solar flux, meaning it forms chromospheric or coronal loops below the height at which gas pressure exceeds magnetic pressure and, thus, does not contribute to the heliospheric magnetic field carried by the solar wind (e.g., Wang and Sheeley Jr, 2003). A fraction of these loops ( $\sim 10$  to 50%, e.g., Arge *et al.*, 2002) do extend high enough to be dragged out by the solar wind, as detailed below. This flux is often termed “open,” as it extends out to form the HMF (note that flux open to the corona may still form closed loops within the heliosphere. See Section 3.1). From photospheric observations alone, it is not possible to discern between open and closed solar magnetic flux and, thus, estimate the magnitude and configuration of the HMF. The observed photospheric magnetic field can, however, be used as a boundary

condition to coronal models. Extrapolation of the photospheric magnetic field requires a complete map of the photospheric field. As all past and present magnetograph instruments are either ground based or in near-Earth space, this means the solar rotation poles are poorly viewed and accruing complete longitudinal coverage requires a full synodic solar rotation,  $\sim 27.27$  days. Thus, photospheric extrapolation is best suited to reconstruction of the steady-state corona and HMF and, consequently, is generally more applicable to solar minimum conditions than the rapidly evolving structures at solar maximum.

The Potential-Field Source-Surface model (PFSS, Schatten *et al.*, 1969; Altschuler and Newkirk Jr, 1969) is the most widely used photospheric extrapolation technique, owing to its simplicity and low computational overhead. It assumes zero current density in the corona, meaning PFSS solutions approximate the minimum energy state of the corona for a given photospheric boundary condition. The inner boundary is the observed photospheric magnetic field, while the outer boundary is the “source surface” where the field is assumed to be radial, typically placed around  $2-2.5 R_S$  in order to best match spacecraft observations (e.g., Hoeksema *et al.*, 1982; Lee *et al.*, 2011). Open solar flux, and hence the HMF, is then defined as any magnetic loop threading the source surface. While the PFSS model has proven invaluable for understanding the solar cycle evolution of the HMF (e.g., see Section 5.4), it should be noted that it does not provide perfect agreement with in situ spacecraft observations of HMF intensity or sector structure, and many features are ad hoc, rather than based on first principles. On the basis of the Ulysses observation of a latitudinal invariance in the strength of the radial HMF (see Section 2.3), a thin current sheet model Schatten (1971) is sometimes added to the PFSS model in order to create a more uniform radial field strength at the source surface (e.g., Wang and Sheeley Jr, 1995).

Photospheric magnetograms can also be used to constrain 3-dimensional magnetohydrodynamic (MHD) models of the corona, such as Magnetohydrodynamics Around a Sphere (MAS) (Linker *et al.*, 1999; Mikić *et al.*, 1999, see also <http://www.imhd.net>) and the Space Weather Modeling Framework (SWMF) (Tóth *et al.*, 2005). Initial conditions are typically derived using the PFSS model and the time-dependent MHD equations then solved to allow the solution to relax to steady state. In general, this produces qualitatively similar results for the heliospheric magnetic field configuration and magnitude to PFSS solutions (Riley *et al.*, 2006a). In principle, the MHD approach allows for a time-dependent inner boundary condition, though at present this involves an ad-hoc manipulation of the photospheric magnetic field and has only been possible for specific event studies (e.g., Linker *et al.*, 2003).

Both PFSS and MHD extrapolations find that open solar flux, the foot points of heliospheric field lines, usually map to dark regions in soft X-ray and EUV images known as coronal holes (e.g., Levine *et al.*, 1977; Wang *et al.*, 1996), which are predominantly confined to the poles at solar minimum (see also Cranmer, 2009). Regions determined to have closed solar magnetic fields are closely associated with the observed locations of coronal bright regions such as helmet streamers, which are confined to the equatorial regions near solar minimum. (Note that alternative interpretations of the source of open solar flux do exist, e.g., Woo (2005).) This pattern was somewhat disrupted during the most recent solar minimum between solar cycles 23 and 24, due to the decreased strength of the polar fields allowing weak equatorial field regions to generate low-latitude coronal holes (Luhmann *et al.*, 2009; Abramenko *et al.*, 2010).

## 2.3 Parker spiral magnetic field

The underlying geometry of the HMF can be understood by considering a completely steady state idealised solar wind with an exactly radial outflow of constant speed, independent of radial and latitudinal position. The footpoints of the magnetic field lines are assumed to be fixed in the photosphere and, hence, to rotate with the Sun. The magnetic field is assumed to be frozen in to solar wind plasma, but to exert no force on it. Under such conditions, the heliospheric magnetic

field becomes twisted into an Archimedean spiral in the solar equatorial plane, as predicted by Parker (1958), and shown schematically in Figure 1.

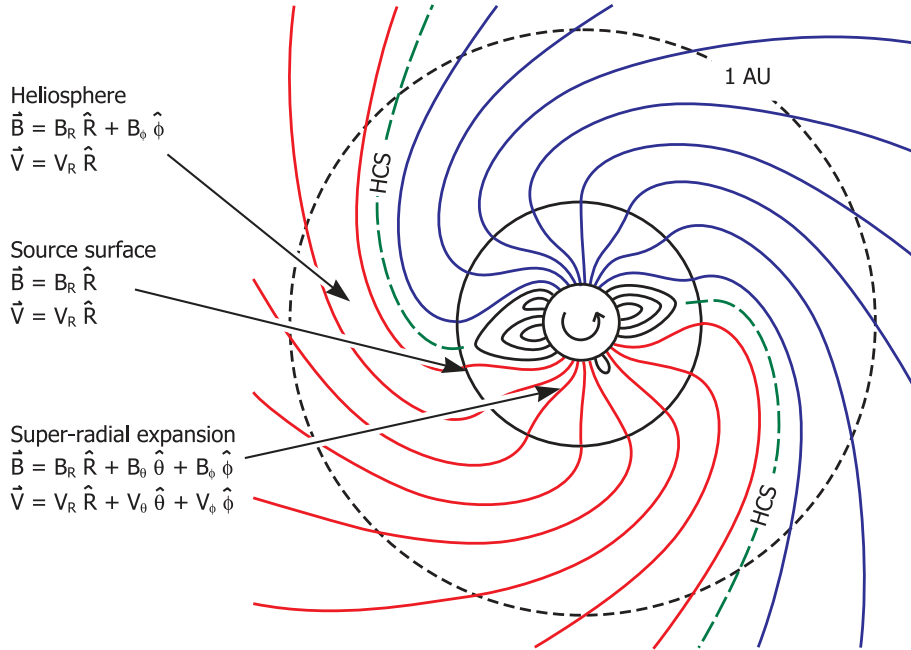


**Figure 1:** A sketch of the steady-state solar magnetic field in the ecliptic plane. Close to the Sun, in a spatial region approximately bounding the solar corona, the magnetic field dominates the plasma flow and undergoes significant non-radial (or super-radial) expansion with height. At the source surface, typically taken to be a few solar radii, the pressure-driven expansion of the solar wind dominates and both the field and flow both become purely radial. In the heliosphere, rotation of the HMF footpoints within a radial solar wind flow generates an azimuthal component of the HMF,  $B_\phi$ , leading to a spiral geometry. Regions of opposite HMF polarity, shown as red and blue lines, are separated by the heliospheric current sheet (HCS), shown as the green dashed line. Image adapted from Schatten *et al.* (1969).

In a constant solar wind flow, magnetic flux conservation requires the radial component of the HMF,  $B_R$ , to fall off as the inverse square of the heliocentric distance,  $R$ . Thus, in a spherical polar coordinate system defined by distance  $R$ , colatitude  $\theta$  and longitude  $\phi$ , we can write

$$B_R(R, \theta, \phi) = B_R(R_0, \theta, \phi_0) \left( \frac{R_0}{R} \right)^2, \quad (1)$$

where  $B_R(R_0, \theta, \phi_0)$  represents the radial component of the magnetic field at colatitude  $\theta$  and footpoint longitude  $\phi_0$  on a solar wind source surface at distance  $R_0$  from the Sun. In the frame of reference corotating with the Sun the plasma streamline and the frozen-in field line coincide. Thus,

$$\frac{B_\phi(R, \theta, \phi)}{B_R(R, \theta, \phi)} = \frac{V_\phi}{V_R} = \frac{-\Omega R \sin \theta}{V_R}, \quad (2)$$

where  $V_R$  is the constant radial solar wind speed and  $V_\phi$  is the azimuthal solar wind speed resulting from the reference frame rotating at an angular speed of  $\Omega$ , the mean solar rotation speed. The  $\sin \theta$  term takes account of the decreasing speed of footpoint motion with latitude as one moves from equator to pole. From Equations (1) and (2) it can be shown that the azimuthal component



of the magnetic field then exhibits a  $1/R$  behaviour with distance:

$$B_\phi(R, \theta, \phi) = -B_R(R_0, \theta, \phi_0) \frac{\Omega R_0^2 \sin \theta}{V_R R}. \quad (3)$$

For completeness, the assumption of an exactly radial solar wind flow gives:

$$B_\theta(R, \theta, \phi) = 0. \quad (4)$$

These equations show that at colatitude  $\theta$ , field lines can be viewed as wrapped around the surface of a cone of half angle  $\theta$  or, alternatively, that the field lines gradually become less tightly wound with latitude until a field line originating from the Sun's rotational pole should be purely radial. In the inertial frame the velocity streamline is radial but the field line remains the same.

Taking a solar wind speed of  $400 \text{ km s}^{-1}$ , typical of 1 AU near the ecliptic, the angle that the heliospheric magnetic field line makes with the radial direction is approximately  $45^\circ$  in the vicinity of the Earth. Early spacecraft observations of the HMF confirmed that the field lines lay approximately in the solar equatorial plane (Coleman Jr *et al.*, 1962) and that the predicted spiral direction was obtained on average (Ness and Wilcox, 1964; Davis Jr *et al.*, 1966). Figure 2 shows magnetic field angle to the radial direction as a function of solar wind speed (after, e.g., Borovsky, 2010). Solid lines show the probability distribution functions calculated from the OMNI dataset, covering 1965–2012. The HMF unwinds at higher speeds, as expected. The vertical dashed lines show the equivalent ideal Parker spiral values, in agreement with the observations. This figure also illustrates the large variability in the HMF direction on the hourly averaged time scale plotted, an important and persistent feature of the HMF over a wide range of time scales.

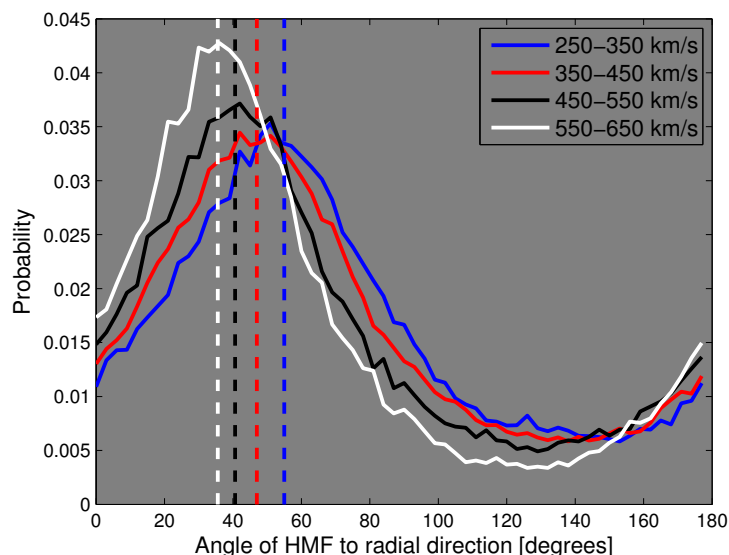


**Figure 2:** Probability distribution functions of heliospheric magnetic field angles to the radial direction for different solar wind speed intervals. The solid curves show hourly OMNI observations of the near-Earth HMF, covering the period 1965–2012. Vertical dashed lines show the equivalent ideal Parker spiral angles for the centre of the speed bins.

The discovery from early observations (e.g., Wilcox and Ness, 1965) that the in-ecliptic HMF is divided into just a few magnetic field polarity sectors in each solar rotation indicates that the HMF

structure in the heliosphere is much simpler than the complexes of activity seen in the photosphere and corona, as indicated schematically in Figure 1. This phenomenon was interpreted (Schulz, 1973) as the dominant dipole and weaker higher order components of the solar field being carried out into the heliosphere by the solar wind, the two polarities of the dipole being separated by the warped heliospheric current sheet (HCS), shown as the green dashed line in Figure 1. The polarity pattern in the heliosphere is discussed in more detail in Section 2.4.

The in-ecliptic HMF, in particular around 1 AU, is well sampled, and the Parker model has been shown to well describe the HMF to a good approximation over a wide range of heliocentric distances: from Helios observations in the inner heliosphere (e.g., Bruno and Bavassano, 1997), Pioneer and Voyager observations out to about  $\sim 8$  AU (Thomas and Smith, 1980; Burlaga *et al.*, 1982), and in the more distant outer heliosphere (Burlaga and Ness, 1993). On the other hand, observations of the high latitude HMF are limited to measurements made by the Ulysses spacecraft (Wenzel *et al.*, 1992), which made three polar orbits of the Sun between launch in 1990 and the end of mission in 2009. At all latitudes, the angle of the HMF to the radial direction was found to closely follow that predicted by Parker, with a general unwinding of the spiral at higher latitudes (Forsyth *et al.*, 2002). Similarly, the HMF, on average, lies on a cone of constant latitude, resulting in no net  $B_\theta$  component. Figure 3 illustrates ideal Parker spiral magnetic fields at latitudes of 0, 30 and 60 degrees (shown as black, blue, and red lines, respectively). However, see Section 4.1 for discussion of deviations from the ideal Parker spiral model.

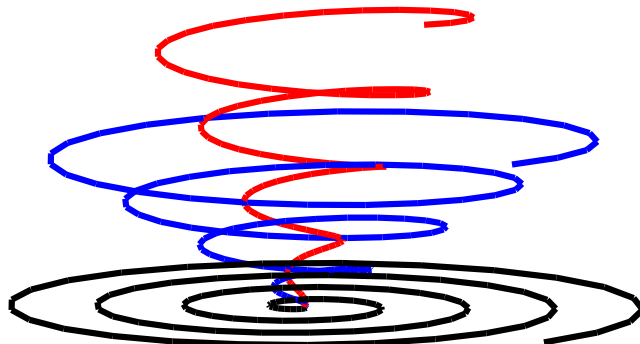


**Figure 3:** Ideal Parker spiral magnetic field lines between 0 and 25 AU for a solar wind speed of  $450 \text{ km s}^{-1}$ . Black, blue, and red lines show heliographic latitudes of 0, 30, and 60 degrees, respectively.

At both solar minimum and solar maximum polar passes, Ulysses observations showed  $R^2 B_R$  to be invariant with latitude (Smith and Balogh, 1995, 2003), contrary to the expectations of PFSS model fields, which approximate a dipolar field at solar minimum. This suggests that close to the Sun (i.e., well within  $10 R_S$ ), the coronal magnetic field undergoes significant non-radial expansion so as to equilibrate tangential magnetic pressure, and hence  $B_R$ , on the solar wind source surface (Suess and Smith, 1996). Consequently, the degree of non-radial expansion undergone by coronal flux tubes can vary considerably depending on the location of the photospheric foot point within a coronal hole. Using a PFSS model of the corona, Wang and Sheeley Jr (1990) found an anticorrelation between flux-tube expansion and resulting solar wind speed, discussed further in Section 2.4. The ‘‘Ulysses result’’ of  $R^2 B_R$  invariance with latitude also means that a measurement of  $B_R$  at any point in the heliosphere is, in principle, sufficient to estimate the total magnetic flux threading a heliocentric sphere at the point of observation, which is directly related to the magnetic flux threading the solar wind source surface, usually referred to as the total unsigned open solar flux (OSF; e.g., Smith and Balogh, 1995; Lockwood *et al.*, 2004, see also Section 5).

## 2.4 Solar minimum: Quasi-dipolar magnetic field

For much of the solar cycle, particularly around solar minimum, the Sun's magnetic field is dominated by its dipolar component, as evidenced by both PFSS solutions to the observed photospheric magnetic field and in situ measurements of the HMF. However, remaining quadrupole distortions are sufficient to induce more complex HMF sector patterns in the ecliptic. The in situ measurements of the Ulysses spacecraft are summarised by Figure 4. The white line in the left-hand panel shows the heliographic latitude of Ulysses overlaid on the sunspot number, shown in black. The dashed white lines bound Ulysses's three fast latitude scans, which each take approximately one year to complete. During these intervals, Ulysses observes solar latitudes between  $80^\circ$  S and  $80^\circ$  N and all solar longitudes owing to solar rotation. The centre column shows the magnetic field polarity observed by Ulysses (red/blue are outward/inward, respectively), mapped back to the source surface and plotted as a function of heliographic latitude and longitude (Jones *et al.*, 2002). The two solar minimum maps show the heliospheric magnetic field is split into two large regions of opposite polarity, approximately aligned with the north and south rotational solar hemispheres. This is the expected signature of nearly rotationally aligned dipolar coronal field, dragged out by the radial solar wind. A weak quadrupolar component can be seen in the slight warping of the HCS and slow solar wind band away from the solar equator. At solar maximum, an approximately dipolar signature is still present, though with a very high tilt to the rotation axis. However, it must be noted that at solar maximum the coronal magnetic field is evolving rapidly, on time scales well below 1-year, the time taken for Ulysses to sample the full solar latitude range. A combination of near-Earth spacecraft observations and PFSS solutions at this time suggest a significant quadrupolar component and that the apparent dipole observed by Ulysses is a result of fortuitous sampling of different latitudes.

At solar minimum, open solar flux and, therefore, the HMF largely maps to polar coronal holes. Thus, assuming the Wang and Sheeley Jr (1990) framework, fast solar wind would be expected from the large-scale unipolar regions over the poles, where the field undergoes little non-radial expansion at high latitudes in comparison to nearer the edges of the streamer belt. Conversely, slower solar wind is expected nearer the solar equator, where opposite magnetic polarities converge to produce helmet streamers and significant non-radial expansion is needed to equalise  $|B_R|$  over the source surface. This solar wind structure was observed by Ulysses (McComas *et al.*, 2003) and is shown in the right-hand column of Figure 4. Note, however, that while flux-tube expansion is extremely useful for identifying the location of slow solar wind, it is unlikely to be the actual mechanism by which it is formed (e.g., McComas *et al.*, 2007, and references therein). At solar maximum, slow solar wind fills much of the heliosphere, as discussed in Section 5.2. In general the sources of the fast wind are better understood than those of the slow wind.

As noted above the large-scale regions of opposite HMF polarity are separated by the heliospheric current sheet (HCS). Near solar minimum, the HCS encircles the Sun close to the rotational equator and hence lies close to the ecliptic plane. Thus, spacecraft in near-Earth space will generally be close in heliolatitude to the HCS and will sample HMF polarities from both polar coronal holes as the Sun rotates, as shown in Figure 6. For a purely dipolar magnetic field typically with at least a small tilt to the rotation axis, a two-sector structure would be expected in the ecliptic plane, as sketched in Figure 1. As the quadrupolar component of the field increases, a more complex sector structure should be observed. Figure 5 shows the observed (top) and PFSS-reconstructed (middle) HMF polarity in near-Earth space as a function of Carrington longitude and time (after, e.g., Wilcox and Ness, 1965; Hoeksema *et al.*, 1982). The bottom panel shows the sunspot cycle. Polarities of OSF estimated by the PFSS extrapolation of the observed photospheric magnetic field agree well with the large-scale magnetic sector structure seen in the heliosphere, throughout the solar cycle. Periods of both two- and four-sector structures are seen. As the HCS is formed by OSF of opposite polarities coming into contact by the non-radial expansion of separate coronal holes,

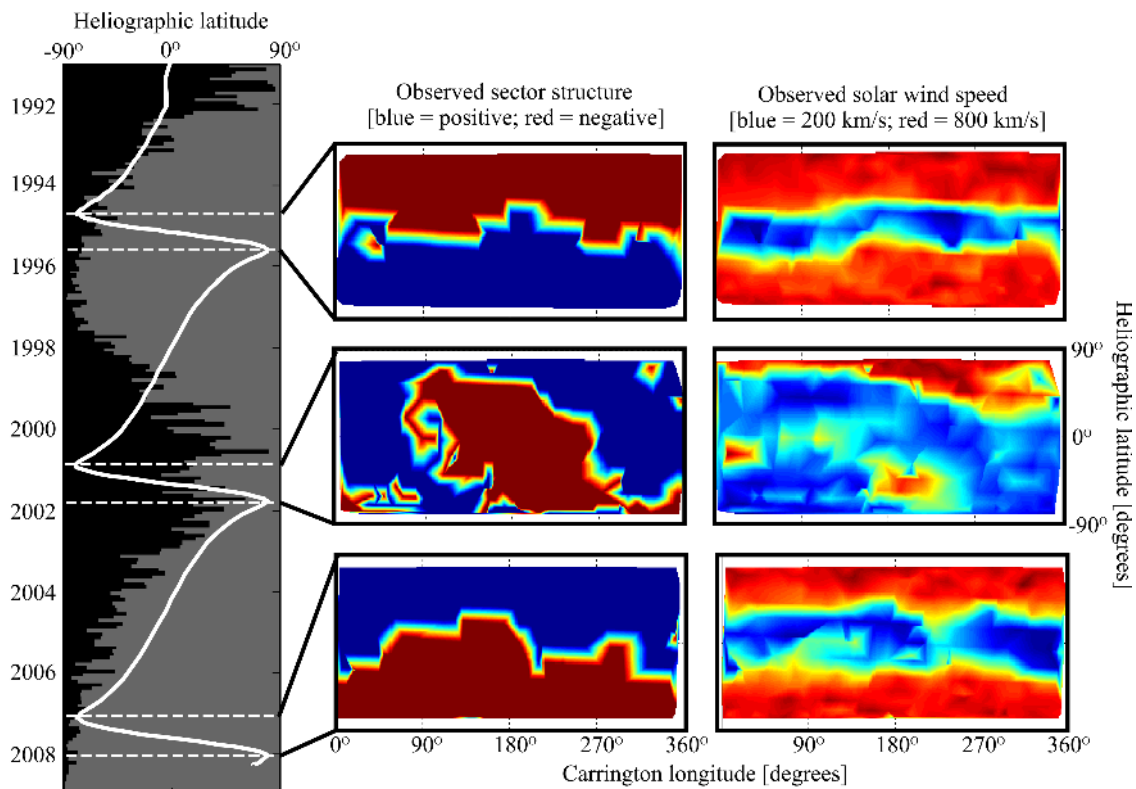


**Figure 4:** A summary of the Ulysses observations. The white line in the left-hand panel shows the heliographic latitude of the spacecraft, overlaid on the sunspot number. The centre and right-hand columns show latitude-longitude maps of Ulysses scan observations made during the three fast-latitude scans, mapped back to the source surface in the same manner as Jones *et al.* (2003). The centre column shows magnetic field polarity, with blue/red dots as inward/outward field. The right-hand column shows solar wind speed, with blue through red showing 200 to 800 km s<sup>-1</sup>. Image adapted from Owens *et al.* (2011a).

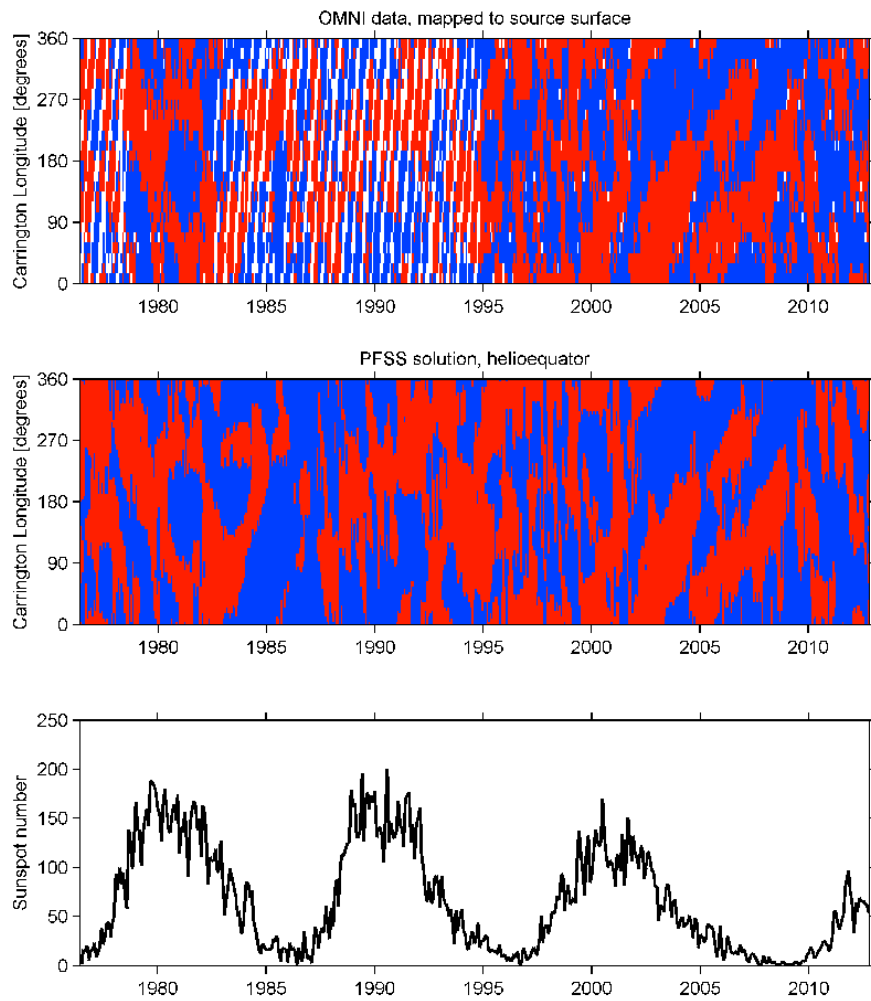


**Figure 5:** Maps of the observed (top) and PFSS-reconstructed (middle) in-ecliptic HMF polarity as a function of Carrington longitude and time. Blue/red indicates inward/outward sectors, respectively. The HMF observed in near-Earth space has been ballistically mapped back to  $2.5 R_S$  for direct comparison with the PFSS output. The bottom panel shows sunspot number.

the HCS maps to helmet streamers and is typically located within slow solar wind (e.g., Figure 4). The two- and four-sector structure have been observed to rotate at different rates: sampled at the Earth the four-sector structure generally follows the 27 day equatorial rotation period while the two-sector structure is often seen to rotate more slowly, at about 28 day period (Svalgaard and Wilcox, 1975).

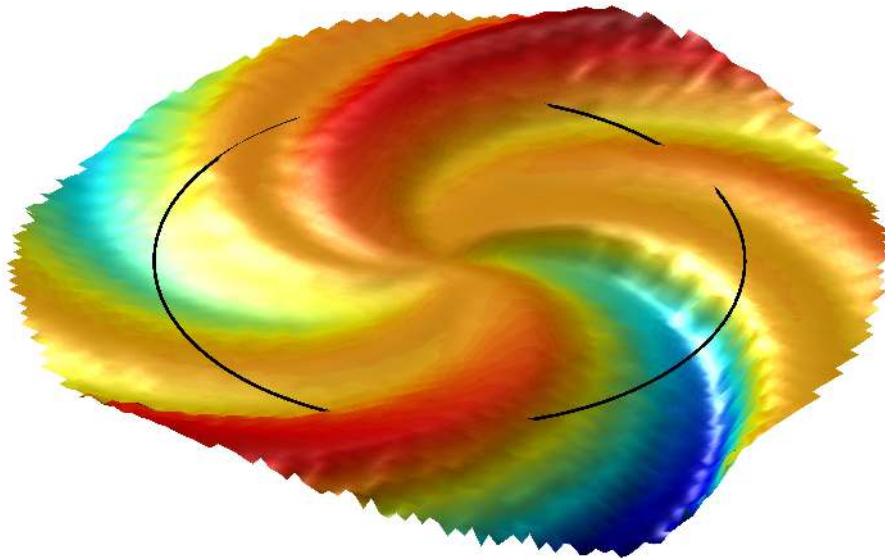


**Figure 6:** The heliospheric current sheet obtained from a coupled corona-heliosphere MHD simulation (Odstrčil *et al.*, 2004) of Carrington rotation 1912, close to the solar minimum at the start of solar cycle 23. At this time, the HCS was primarily about the heliographic equator, but red/blue colours show warps of the HCS which extend approximately 10 degrees above/below the equator. The thick black line shows Earth's path through the HCS. Warping of the HCS results in six major HCS crossings during this Carrington rotation. Note that the thinning of the black line in the upper-left corner indicates a period when Earth skims the HCS for an extended period, which may result in numerous HCS crossings from fine scale structure not revealed by these simulation results.

## 2.5 Stream interaction regions

Inclination of the solar magnetic axis to the solar rotation axis, as well as warps in the streamer belt, combined with the rotation of solar wind sources with the Sun, results in fast and slow solar wind successively entering the heliosphere at a fixed longitude in heliospheric coordinates, as shown in Figure 7. In such instances, fast wind (red) will catch up with slow wind ahead of it (blue) and the stream interface (SI) will take the form of a spiral front (black). The region of solar wind compression and deflection is referred to as the stream interaction region (SIR). In the quasi-steady state regime, SIRs will corotate with the Sun, and are thus referred to as corotating interaction regions (CIRs, Smith and Wolfe, 1976; Pizzo, 1991; Gosling and Pizzo, 1999; Crooker *et al.*, 1999). In near-Earth space, CIRs are most commonly observed during the declining phase of the solar cycle, when there is typically a quasi-stable dipolar corona with significantly inclination to the rotational axis.

In the rest frame of the solar wind, both fast and slow wind flow in toward the SI. As the HMF is frozen to the plasma flow, neither fast nor slow wind can pass through the SI and are deflected along it. This is achieved by disturbance waves propagating anti-sunward into the slow

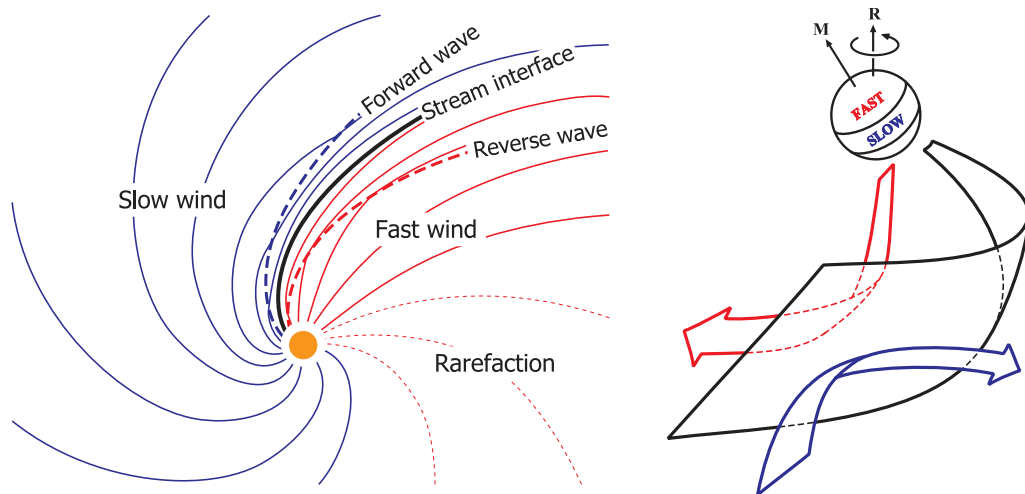


**Figure 7:** A sketch of a stream interaction region. *Left:* Looking down on the ecliptic plane. Magnetic field lines within fast (slow) wind, shown in red (blue), become aligned with the stream interface by the reverse (forward) wave. *Right:* a view from Earth. The magnetic axis, M, and therefore the wind speed belts, are inclined to the rotation axis, R. The point in the heliosphere at which fast wind is able to catch up to the slow wind ahead of it is the stream interface (SI), which forms a spiral front in the heliosphere, shown as the black-outlined curved surface. In the frame of reference of the SI, both fast and slow wind flow toward the SI. Fast (slow) wind, shown by the red (blue) arrow, is slowed (accelerated) and deflected along the SI in the direction counter to (along) solar rotation. Right panel adapted from Pizzo (1991).

solar wind and sunward (in the plasma rest frame) into the fast wind. Figure 8 shows a CIR observed by Ulysses at 5.1 AU, just below to the ecliptic plane. The forward and reverse waves, shown as blue and red vertical lines, respectively, have steepened into shock fronts, which typically occurs at heliocentric distances larger than 2 AU (Smith and Wolfe, 1976). Within the interaction region, bounded by the red and blue lines, the magnetic field intensity and plasma density are enhanced by compression. Figure 7, based on the model of Pizzo (1991), shows how inclination of the stream interface means solar wind flow is systematically deflected along the SI, with fast (slow) solar wind deflected in the direction counter to (along) the solar rotation direction and poleward (equatorward) with respect to the heliographic equator. The poleward and equatorward deflections being confirmed observationally from Ulysses data by Gosling *et al.* (1993b).

As the HMF is frozen to the solar wind flow, it should be dragged in the same sense as the deflected flow within an interaction region. Clack *et al.* (2000) found that this expected large scale correlation between the flow and the magnetic field was hard to extract from the general variability of the magnetic field direction. However, due to the compression of the HMF within the interaction region, the varying magnetic field is forced to lie in a plane approximately parallel to the SI. As a consequence of the relationship between the HCS and the coronal streamer belt, the HCS is located at the centre of the slow solar wind band near the Sun. Indeed, the HCS is often observed to be embedded within SIRs and CIRs (Gosling and Pizzo, 1999). As the forward wave/shock propagates into the slow solar wind ahead of a CIR it can eventually overtake the HCS boundary, making it more likely for the HCS to be embedded within a CIR with increasing distance from the Sun (Thomas and Smith, 1981). In Figure 8, the location of the HCS is shown by the green dashed line. Behind the compressed interaction region, at the trailing end of the high-speed stream the fast solar wind runs away from the slow solar wind behind it, creating a rarefaction region in which the magnetic field intensity and plasma density are reduced, and the solar wind speed monotonically declines. Behind the SI and within the rarefaction region it is often noticed

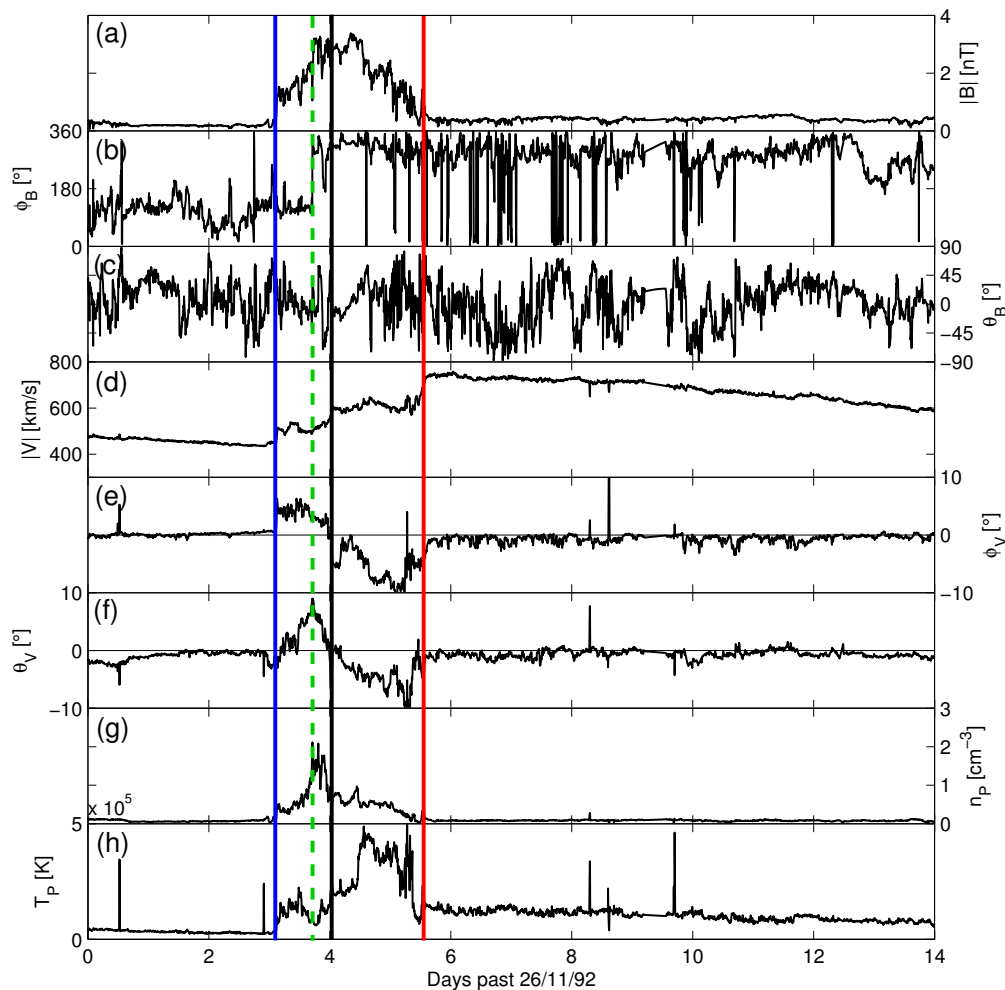


**Figure 8:** A corotating interaction region observed by Ulysses just below the ecliptic plane ( $-20^\circ$  latitude) at 5.1 AU. Panels, from top to bottom, show: (a) magnetic field intensity, the angle of the magnetic field (b) in the R-T plane (i.e., the plane containing the ideal Parker spiral magnetic field, in this case, close to the ecliptic plane) and (c) out of the R-T plane, (d) the solar wind speed, the angle of the solar wind flow (e) in and (f) out of the R-T plane, (g) the proton density, and (h) proton temperature. The black vertical line shows the stream interface. The red (blue) vertical line shows the reverse (forward) shock propagating into the fast (slow) solar wind behind (ahead) of the SI. The green dashed line shows the location of the heliospheric current sheet.



that the magnetic field components have higher variance. This is because the presence of large amplitude Alfvén waves is a typical property of the fast solar wind (e.g., [Belcher and Davis Jr, 1971](#)).

## 2.6 Outer heliosphere

With the Voyager 1 spacecraft having recently passed the heliopause ([Gurnett \*et al.\*, 2013](#)) and Voyager 2 close behind, our understanding of the outer heliosphere is evolving rapidly. This section contains a very brief summary of the outer heliosphere magnetic field. For a more comprehensive discussion of these topics, [Zank \(1999\)](#) and [Linsky \(2009\)](#) provide excellent, in-depth reviews of the distant heliospheric structure, while [Balogh and Jokipii \(2009\)](#) review the heliospheric magnetic field in the heliosheath.

The global-scale structure of the heliosphere and its interaction with the local interstellar medium (LISM) can be largely understood through magnetohydrodynamic simulations (e.g., [Zank, 1999](#), and references therein), though they must include the effect of heliospheric pickup ions, produced by the photoionisation of neutral atoms (see [Section 3](#)), as they dominate the solar wind momentum flux past  $\sim 10$  AU. A sketch of the expected plasma and magnetic field boundaries is shown in [Figure 9](#). The motion of the Sun and heliosphere relative to the LISM is  $23 \text{ km s}^{-1}$  ([Linsky \*et al.\*, 1995](#)). Given the uncertainty in the LISM magnetic field strength and orientation, there is still some debate about whether this motion is super Alfvénic and, thus, results in a standing bow shock within the LISM. Recent observations from the IBEX mission (see [Section 3](#)), however, argue that the orientation of the LISM magnetic field is such that the interaction is sub-magnetosonic ([McComas \*et al.\*, 2012](#)). Much like the interaction of the Earth’s magnetosphere with the solar wind, the heliopause is expected to be compressed on the LISM inflow side and extended on the downflow side. Unlike the magnetopause, however, the super Alfvénic solar wind outflow produces a standing termination shock inside the heliopause, which compresses, slows and deflects the solar wind flow. The Voyager 1 spacecraft crossed the termination shock in December 2004 at 94 AU ([Stone \*et al.\*, 2005](#)), with Voyager 2 making its entry into the heliosheath in August 2007 at 84 AU ([Stone \*et al.\*, 2008](#)). Voyager 2 started seeing enhancements in energetic particles at 76 AU, suggesting the termination shock is non-spherical, which allows particles to escape from the shock, back down the Parker spiral HMF ([McComas and Schwadron, 2006](#)). Inclination in the magnetic field of the local interstellar medium relative to that of the heliosphere may lead to further asymmetries near the heliopause ([Schwadron \*et al.\*, 2011](#)). Voyager 1 recently encountered a region of flow stagnation, where the solar wind speed reached zero ([Krimigis \*et al.\*, 2011](#)), before measuring an electron density enhancement consistent with the interstellar medium in April 2013 ([Gurnett \*et al.\*, 2013](#)). The full implications of these observations are still being assessed and will be included in a future revision of this review.

Inside the termination shock, the HMF is generally well described by the Parker spiral model, however, there is some debate about whether the fall-off in magnetic field intensity is faster than predicted. Note that the radial magnetic field,  $B_R$ , decreases as the square of the heliocentric distance [[Equation \(1\)](#)] and can be both positive and negative, meaning it is technically challenging to make measurements of the outer-heliosphere  $B_R$  with sufficient accuracy to test the Parker model. The magnetic field intensity,  $B$ , is a scalar quantity, so can be averaged over long time periods. Analysis of the Pioneer 10 and 11 data suggested  $B$  decreases by approximately 1% per AU more than predicted by the Parker model ([Winterhalter \*et al.\*, 1990](#)). The existence of such a “flux deficit” ([Thomas \*et al.\*, 1986](#)) is disputed by [Burlaga \*et al.\* \(2002\)](#), who argue that the Voyager observations are consistent with the Parker model within observational uncertainty, if both the solar cycle variation of the solar source  $B$  and time/latitude variations in solar wind speed are accounted for.

Assuming the observed latitudinal invariance in  $B_R$  in the inner heliosphere, the  $\sin\theta$  term

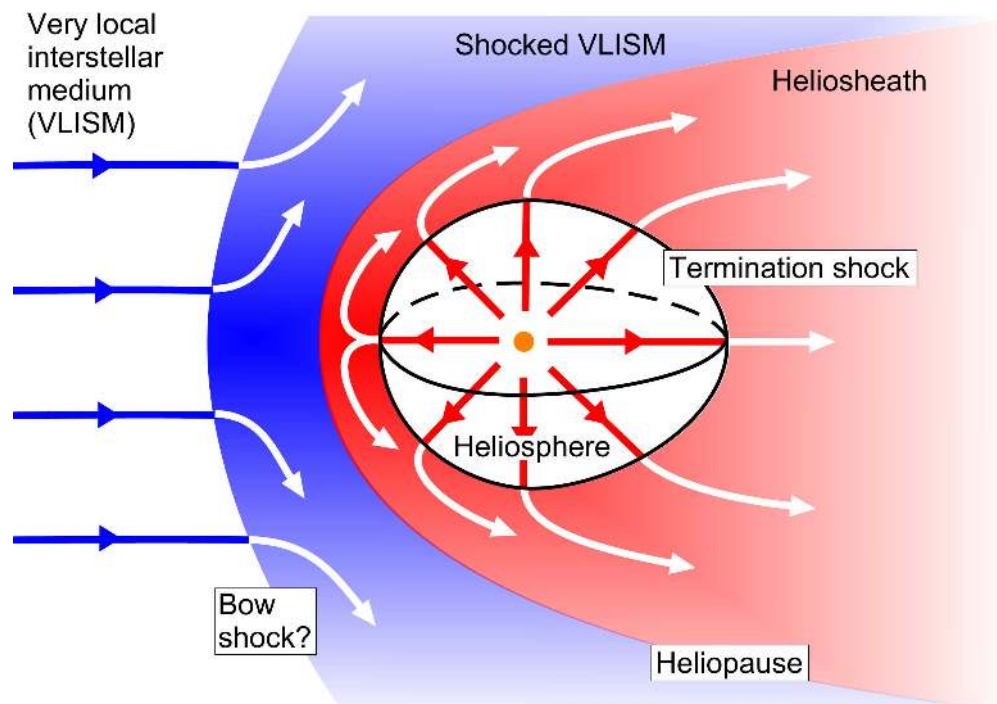


**Figure 9:** A cartoon of the global structure of the heliosphere. The solar wind flows radially away from the Sun. As the flow is supersonic, a termination shock forms inside the heliopause, to slow and deflect the solar wind inside the heliosheath. Outside the heliopause, the very local interstellar medium (VLISM) is deflected around the heliosphere. Depending on the strength and orientation of the magnetic field within the VLISM, this interaction may or may not involve a standing bow shock.

in  $B_\phi$  [Equation (3)] means  $B$  in the outer heliosphere should be stronger near the equator than the poles. Pioneer and Voyager spacecraft, however, did not find strong evidence of latitudinal gradients in  $B$  (Winterhalter *et al.*, 1990). There are a number of possible explanations for these observations. The confinement of SIRs to low latitudes at solar minimum means that the HMF has a tendency to become more radial than the Parker model predicts. Furthermore, the excess plasma pressure produced by heating at the SIR forward/reverse shocks could lead to a meridional expansion of the HMF, transporting flux to higher latitudes, in agreement with the small poleward plasma flows detected by Voyager (e.g., Richardson and Paularena, 1996). Alternatively, at solar minimum, the Kelvin–Helmholtz instability could act between the high-latitude fast wind and the low-latitude slow wind to generate a channel of vortices to drive such plasma flows and, hence, transport HMF (Burlaga and Richardson, 2000).

The shorter time-scale dynamics of the outer heliospheric HMF are dominated by merged interaction regions (MIRs, e.g., Burlaga *et al.*, 2003; Hanlon *et al.*, 2004); huge structures of compressed magnetic field and plasma which form from coalescing solar wind structures such as CIRs and ICMEs. The early formation of these structures can be observed even at 1 AU, where they can result in prolonged and severe geomagnetic effects. In the outer heliosphere, they can produce significant (if transient) deviations to the Parker spiral magnetic field. (See also Section 4.2.) MIRs also provide strong barriers to galactic cosmic ray propagation and in extreme cases may produce a significant disturbance to the structure of the heliopause and termination shock.

### 3 Particle Probes of the HMF

While in situ magnetometer measurements can make extremely accurate observations of the local magnetic field strength and orientation, information about the global heliospheric magnetic field topology, particularly HMF connectivity to the solar surface, can be probed through energetic particle observations.

#### 3.1 Suprathermal electrons

Suprathermal electrons (STEs) have energies well above the thermal plasma (e.g.,  $> 70$  eV), allowing them to stream along the HMF and carry the heat flux away from the Sun (Feldman *et al.*, 1975; Rosenbauer *et al.*, 1977). As the STEs move out into the heliosphere, a strong STE field-aligned beam, or “strahl,” is formed by conservation of magnetic moment. This strahl serves as an effective tracer of heliospheric magnetic field topology. As STEs move much faster along magnetic fields than the bulk plasma flow, they also act as near-instantaneous indicators of magnetic connection to the Sun.

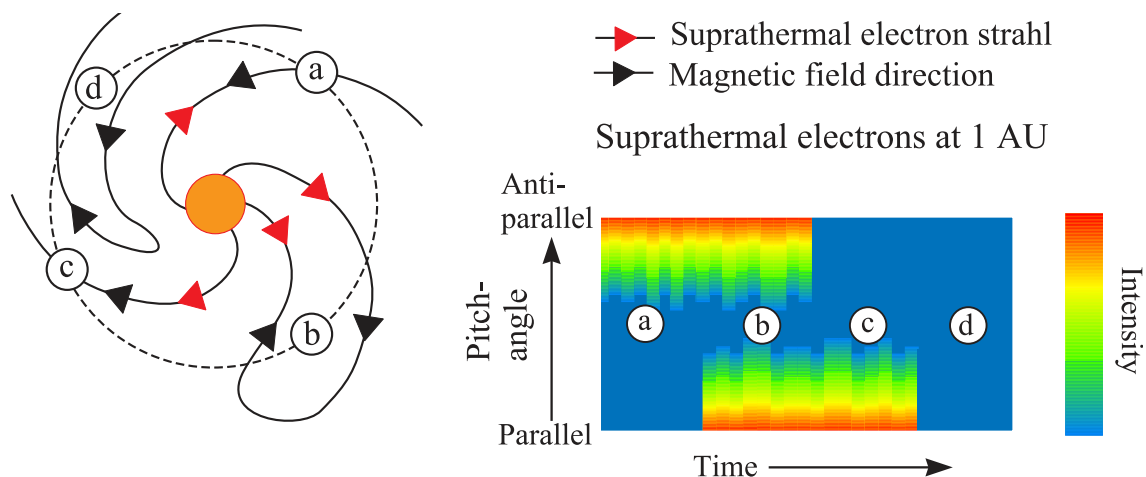


**Figure 10:** A sketch of heliospheric magnetic topology inferred from suprathermal electron observations. *Left panel:* A view of the ecliptic plane, with magnetic field lines shown as black arrows and the anti-sunward suprathermal electron flux shown as red arrows. *Right panel:* The STE pitch-angle distribution seen by a spacecraft in near-Earth orbit. At (a), the field is part of an inward-polarity sector, so the STE strahl is anti-parallel to the field. Similarly, at (c), the outward sector results in a parallel strahl. At (b), the magnetic field is connected to the Sun at both ends, resulting in both parallel and anti-parallel strahls, or counterstreaming. At (d), there is no solar connection, so no strahl is seen.

Figure 10 shows a sketch of the relation between heliospheric magnetic topology and suprathermal electrons. The left panel shows a view of the ecliptic plane, with magnetic field lines shown as black arrows and the anti-sunward STEs shown as red arrows. The right panels shows the expected STE pitch-angle distribution seen by a spacecraft in near-Earth orbit. “Open” heliospheric magnetic flux has a single connection to the Sun, as shown at (a) and (c), and will therefore result in a single strahl (Feldman *et al.*, 1975; Rosenbauer *et al.*, 1977). A strahl parallel or anti-parallel to the HMF reveals the polarity of the magnetic foot point connected to the Sun, regardless of any “folding” or twisting of the field between the Sun and point of observation (Crooker *et al.*, 2004b). Thus at (a), the field is part of an inward-polarity sector, so the STE strahl is anti-parallel to the field. Similarly, at (c), the outward sector results in a parallel strahl. At (b), the HMF forms a closed loop, with the magnetic field connected to the Sun at both ends. Thus, while the

magnetic field threads the source surface to form open solar flux, it is closed in the heliosphere. This results in both parallel and anti-parallel strahls (Gosling *et al.*, 1987), commonly referred to as bi-directional electrons (BDEs) or counterstreaming electrons (CSEs). This signature may only be present for newly added heliospheric loops, as the apex of a loop will continue to move anti-sunward meaning the loop length will increase such that the CSE signature is lost by pitch-angle scattering (Hammond *et al.*, 1996; Maksimovic *et al.*, 2005; Owens *et al.*, 2008b). This CSE signature is closely correlated with interplanetary coronal mass ejections (Gosling *et al.*, 1987, see also Section 4.2). It should be noted, however, that CSEs can also result from open heliospheric flux when STEs are reflected at discontinuities, particularly strong shocks (Gosling *et al.*, 1993a), and through pitch-angle focussing and mirroring on open field lines (Gosling *et al.*, 2001; Steinberg *et al.*, 2005). Thus, care must be taken when interpreting STE data in terms of magnetic connectivity.

Finally, at (d), the HMF has no connection to the photosphere, forming a disconnected loop in the heliosphere. No strahl is expected on such a flux system, and periods of “heat flux dropouts” (HFDs; McComas *et al.*, 1989) or, more accurately, “electron dropouts” (EDs; Owens and Crooker, 2007) are expected. However, they are observed to be extremely rare in solar wind observations (Pagel *et al.*, 2005, 2007). Note that this does not necessarily mean that the disconnection of heliospheric flux is uncommon, just that the signature of disconnection is only fleetingly observable at 1 AU (see Owens and Crooker, 2007, for more detail).

### 3.2 High-energy particles

While suprathermal electrons are ubiquitous in the solar wind, there are also intermittent bursts of much higher energy particles, both electrons and ions, which result from particle acceleration at solar flare sites and at shock fronts driven by solar eruptions and stream interaction regions (SIRs). As the flare-associated impulsive solar energetic particles (SEPs) have distinct launch times, the dispersion in arrival times of particles of different energies can provide information about the length of the field line connecting the observer and the source (e.g., Larson *et al.*, 1997; Chollet and Giacalone, 2011; Kahler *et al.*, 2011). When the particle acceleration site can be reliably determined (e.g., using extreme ultra-violet or soft X-ray observations of a flare), the spatial connection between the observer and the Sun can also be inferred. Energetic particles accelerated at SIR-driven shock fronts (see Section 2.5) have been particularly useful for understanding changing connectivity of the HMF to the photosphere (Fisk, 1996, see also Section 5.4).

Energetic particles from non-solar sources can also reveal information about the large-scale heliospheric magnetic field. Energetic electrons released by the Jovian magnetosphere (Teegarden *et al.*, 1974; Chenette *et al.*, 1974) provide a point source in the heliosphere which can be used to infer magnetic connectivity to Jupiter and, hence, the large-scale structure of the HMF (Chenette, 1980; Moses, 1987; Owens *et al.*, 2010). Galactic cosmic rays (GCRs) (e.g., Usoskin, 2013, and references therein), which originate outside the solar system, are near isotropic. Thus, changes in GCR flux can reveal information about the large-scale HMF, particularly the total open solar flux (OSF) and heliospheric current sheet orientation (e.g., Ferreira and Potgieter, 2003; Alanko-Huotari *et al.*, 2007, see also Section 5.5.3). Cosmic-ray intensity in the heliosphere rises and falls in anticorrelation with the OSF and, hence, shows a strong 11-year solar cycle variation. Cosmic-ray intensity, however, also shows a 22-year cycle (Webber and Lockwood, 1988; Smith, 1990), with alternate cycles displaying “peak-” and “dome-like” variations. This is primarily due to differing cosmic ray drift patterns in alternate global solar magnetic polarities (Jokipii *et al.*, 1977), though there is some evidence that the OSF and latitudinal extent of the heliospheric current sheet are enhanced during odd-numbered solar cycles relative to even ones, which may lead to direct modulation of cosmic rays by differing heliospheric structure (Cliver and Ling, 2001; Thomas *et al.*, 2013).

While less directly relevant to this review, we note there are a host of other non-solar energetic particles present in the heliosphere which are of great interest to a range of scientific areas. Pickup ions are formed when neutral particles become ionized and entrained in the solar wind and, hence, reveal information about both the neutral interstellar medium and the inner heliospheric dust distribution (see [Gloeckler \*et al.\*, 2001](#), for an excellent review of the subject). As pickup ions can contribute as much as 10% of the abundance of solar wind ions in the outer heliosphere, they can affect solar wind dynamics at large heliocentric distances. Energetic neutral atoms (ENAs), on the other hand, are high-energy charged particles which charge exchange with the solar wind to become neutral. As they are demagnetised, they travel large distances undisturbed, enabling remote sensing of magnetospheres or distant heliospheric structure, such as the heliopause ([Gruntman, 1997](#)). The Interstellar Boundary Explorer (IBEX) mission ([McComas \*et al.\*, 2009](#)) is currently mapping the structure of the heliopause through ENA imaging, as discussed in Section [2.6](#).

## 4 Transient and Fine-scale Structure

### 4.1 Deviations from the Parker model

While the Parker model describes the HMF remarkably well, there are a number of “second-order” alterations or additions required to fully explain observations. One such observation is the existence of shock-accelerated particles at latitudes higher than where CIR shocks are located. In the declining phase of the solar cycle, Ulysses observed CIRs to be confined to within  $40^\circ$  of the solar equator, about  $10^\circ$  greater than the  $\sim 30^\circ$  maximum latitude of the HCS at the time, but the energetic protons and electrons associated with CIR shocks were observed at much higher latitudes (Roelof *et al.*, 1997). While solar wind particles are typically frozen to field lines, one possible explanation is that these more energetic particles effectively diffuse across the magnetic field as a result of scattering off magnetic waves and inhomogeneities (Kóta and Jokipii, 1995).

Alternatively, if the photospheric connectivity of heliospheric field lines changes in a systematic fashion, particles accelerated at CIRs close to the HCS could be expected at high latitudes without the need for strong cross-field diffusion. Such a framework was described by Fisk (1996). It results from combining a number of observations of the solar magnetic field, most importantly, the photospheric plasma and magnetic field are known to rotate differentially with latitude, from a rotational period of approximately 25 days at the equator, to over 30 days in the polar regions. Coronal holes, on the other hand, are observed to rotate rigidly about the rotation axis but with an axis of symmetry which is tilted with respect to the rotation axis (e.g., Bird and Edenhofer, 1990, and references therein). The non-radial overexpansion of the magnetic field within coronal holes described at the end of Section 2.3 also takes place about this symmetry axis. If this symmetry axis and rotational axis are aligned, HMF footpoints drift around the rotation axis resulting in a Parker-like heliospheric field in which the HMF traces out cones of constant latitude even if the field lines are rooted at a higher latitude in the photosphere. If, however, the symmetry axis of the magnetic structure is inclined to the rotational axis, the HMF becomes more complex and a field line from a particular moving photospheric source can make large excursions in latitude over time in the heliosphere due to experiencing different amounts of overexpansion in the corona. A further consequence of magnetic inclination to the rotation axis is that reconnection between the open HMF within coronal holes and closed coronal loops at the edges of coronal holes (referred to as “interchange reconnection,” e.g., Crooker *et al.*, 2002) allows the HMF footpoints to saltate across the photosphere against differential rotation (Nash *et al.*, 1988; Wang and Sheeley Jr, 2004). See Fisk *et al.* (1999) for more detail.

The effects of the above model should be most systematic in the stable tilted dipole configuration of the solar corona often encountered in the declining and minimum phases of the solar cycle, such as was characteristic of the 1992–1997 Ulysses data. Attempts have been made to detect systematic latitudinal components in the Ulysses HMF data (Zurbuchen *et al.*, 1997; Forsyth *et al.*, 2002) but it was found likely that the amplitude of the signal would be too small to stand out from the general variability of the field. Alternative observational evidence for the resulting deviations from the Parker model can be found in rarefaction regions behind CIRs, where the HMF is found to be systematically more radial than an ideal Parker spiral for the observed solar wind speed (Murphy *et al.*, 2002). This has been interpreted as the changing solar wind speed at the HMF footpoint (Schwadron, 2002), which could be expected if the HMF footpoint moves across the coronal hole boundary at the trailing edge of the fast stream as a result of differential rotation. Indeed, a similar mechanism has been proposed as the source of the slow solar wind (Fisk, 2003).

Solar wind intervals have also been identified in which the HMF is Parker spiral-aligned, but the suprathermal electron strahl is directed toward the Sun (Kahler *et al.*, 1996; Crooker *et al.*, 2004b, and references therein). This must result from the HMF being locally inverted, most likely as a result of interchange reconnection in the corona opening up a previously closed coronal loop

(Owens *et al.*, 2013), possibly a further signature of the circulation of the HMF.

Stimulated by asymmetries noted in the latitudinal gradients of cosmic rays in 1995 solar minimum Ulysses observations, there has been continuing interest as to whether there is a north-south asymmetry present in both the solar and heliospheric magnetic fields. It was noted at the time that these results could be explained by a  $\sim 10^\circ$  southward displacement of the heliomagnetic equator and, hence, the heliospheric current sheet (e.g., Simpson *et al.*, 1996). Although initial analysis of Ulysses magnetic field data did not support such a large displacement, Smith *et al.* (2000) showed that Wind data in the ecliptic were consistent with a  $\sim 10^\circ$  displacement at this time, the effect at Ulysses being masked by temporal changes. Subsequent analysis of HMF data at 1 AU (Mursula and Hiltula, 2003) and at Ulysses (Erdős and Balogh, 2010) have yielded results consistent with a long term trend of a few ( $\sim 2-3$ ) degrees southward displacement of the HCS. During the Ulysses mission, this displacement has been consistently southward, independent of the reversals in the solar magnetic dipole polarity in alternate solar cycles. As discussed in the review of Smith (2008), the interpretation and comparison of these and similar studies requires care in separating spatial and temporal effects.

## 4.2 Interplanetary coronal mass ejections

Coronal mass ejections (CMEs) are huge eruptions of solar plasma and magnetic field. As CME initiation and release frequently involves magnetic reconnection, CMEs are often spatially and temporally collocated with solar flares, though it is now clear that flares do not trigger CMEs (Harrison, 1995). CMEs move out through the corona and into the heliosphere where fast (slow) CMEs are accelerated (decelerated) towards the ambient solar wind speed (e.g., Gopalswamy *et al.*, 2000; Cargill, 2004). These interplanetary CMEs (ICMEs) can be observed both remotely with white-light heliospheric imagers as density perturbations (e.g., Davis *et al.*, 2009) and directly with in situ magnetic field and particle detectors. ICMEs produce the largest deviations from the Parker spiral magnetic field and are the primary source of strong meridional HMF in the near-Earth solar wind, making ICMEs particularly geoeffective (e.g., Gosling, 1993; Schwenn, 2006, and references therein). The out-of-ecliptic magnetic field can result both from the ICME structure itself (see Section 4.2.1) and from distortion of the ambient HMF (e.g., Jones *et al.*, 2002, see also Section 2.5).

There are a number of plasma, magnetic field, compositional and charge-state signatures used to identify ICMEs from in situ data, though no one signature is either necessary or sufficient for classification. Ion charge state and elemental abundance signatures are generally consistent with CMEs forming in the hotter corona, below the bulk solar wind acceleration height (e.g., Gloeckler *et al.*, 1999; Lepri and Zurbuchen, 2004). Plasma density and pressure are usually lower than the bulk solar wind, suggesting ICMEs undergo greater expansion than the bulk solar wind (e.g., Cane and Richardson, 2003). See Neugebauer and Goldstein (1997) and Wimmer-Schweingruber *et al.* (2006) for thorough reviews of ICME signatures and their implications for the formation and evolution of ejecta. In this review, we concentrate on the magnetic signatures of ICMEs, and how ICMEs relate to the HMF in general.

### 4.2.1 Magnetic clouds

Magnetic clouds (MCs) are a subset of ICMEs primarily characterised by a large-scale, smooth rotation in the magnetic field direction, and are typically associated with an increase in field magnitude and a decrease in small-scale field variance (Burlaga *et al.*, 1981; Klein and Burlaga, 1982). These signatures have been interpreted and modeled as a magnetic flux rope (Burlaga, 1988; Lepping *et al.*, 1990). Figure 11 shows an example of a magnetic cloud, observed by the Wind and ACE spacecraft in August 1998. Approximately 5 days of data are shown, with the MC

boundaries shown as the solid vertical lines. The second panel from the top shows the magnetic field magnitude, which is significantly enhanced above that in the ambient solar wind. The following two panels show the in- and out-of-ecliptic plane angles of the magnetic field, respectively. The smooth rotation in the magnetic field direction is clearly identifiable, resulting in large out-of-ecliptic magnetic fields at the front and rear portions of the MC. It's likely such magnetic clouds are the largest events in a spectrum of flux-rope associated solar ejecta (Moldwin *et al.*, 2000; Rouillard *et al.*, 2011).

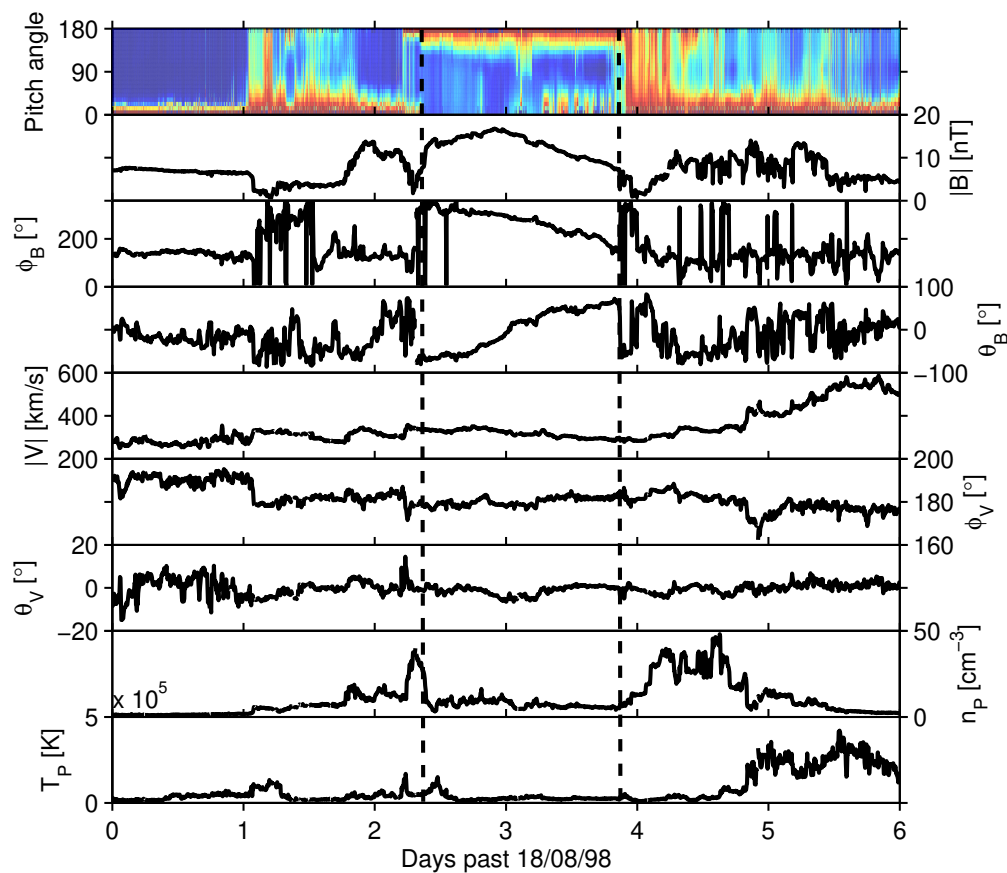


**Figure 11:** An example of a magnetic cloud, observed by the Wind and ACE spacecraft in August 1998. Approximately 5 days of data are shown, with the MC boundaries shown as the solid vertical lines. The panels, from top to bottom, show: the suprathermal electron pitch-angle distribution, the magnetic field magnitude, the in- and out-of-ecliptic magnetic field angles, the solar wind flow speed, the in- and out-of-ecliptic flow angles, the proton number density, and the proton temperature.

MCs comprise between a third (Gosling, 1990) to a half (Cane and Richardson, 2003) of all ICMEs in near-Earth space, with some evidence of this fraction varying with the solar cycle (Riley *et al.*, 2006b). At present, it is unclear whether or not all CMEs involve erupting flux ropes, but the signature is simply not seen in in situ observations because of sampling effects, in-transit distortion, etc. (e.g., Jacobs *et al.*, 2009). Although constituting a minority of total ICMEs observed, MCs have received considerable attention for two reasons. Firstly, they drive the largest geomagnetic disturbances (Gosling, 1993; Richardson *et al.*, 2002). Secondly, fitting a flux rope model to the single-point in situ data allows estimation of the large-scale magnetic properties of ICMEs to be



estimated, notably the local flux-rope orientation and total magnetic flux content, information unobtainable by other methods and/or observations.

#### 4.2.2 Relation of CMEs to the HMF

The total CME mass flux, as estimated from coronagraph observations, is only a minor contribution to the solar wind (Webb and Howard, 1994). Similarly, the magnetic flux carried by a single magnetic cloud is  $\sim 10^{12} - 10^{13}$  Wb (Lynch *et al.*, 2005; Owens, 2008), only a few percent of the estimated total open solar magnetic flux at any time ( $\sim 10^{15}$  Wb, e.g., Owens *et al.*, 2008a). This is in rough agreement with the small fraction of time the near-Earth solar wind can be attributed to recognisable ICME material (Richardson *et al.*, 2000). However, while a single CME is unlikely to have a significant contribution to the total open solar flux, the net CME contribution also depends on the time for which CME magnetic flux remains connected to the Sun, as discussed in Section 5.4. Indeed, there are a number of observations which suggest CMEs are intrinsically linked with the large-scale evolution of the HMF, as discussed here.

Particularly during solar minimum, when the streamer belt and heliospheric current sheet coincide, magnetic clouds are frequently encountered at magnetic sector boundaries. In such instances, the normally sharp transition from inward to outward magnetic polarities associated with a crossing of the HCS instead takes the form of a smooth rotation in the magnetic field direction associated with the passage of the MC's flux rope (Crooker *et al.*, 1998a). Clearly, the magnetic cloud polarity is determined by the large-scale solar magnetic field orientation and may be a means by which the large-scale field evolves, shifting the location of the sector boundary in response to a change in the photospheric magnetic flux (Crooker *et al.*, 1998b, see also Section 5.4). Note, however, that many CMEs do not result in a permanent change to the HCS position (Zhao and Hoeksema, 1996). The relation between the large-scale solar magnetic field and ICMEs is further evidenced by the observed solar-cycle and hemispheric trends in magnetic cloud orientations and polarities. In-ecliptic observations of magnetic clouds show that their orientation and polarity follows the Hale law of sunspot polarity (Hale and Nicholson, 1925), where the polarity of the leading (in the sense of solar rotation), lower-latitude sunspot is the same as the dominant hemispheric polarity at the start of the solar cycle (Bothmer and Rust, 1997; Bothmer and Schwenn, 1998; Mulligan *et al.*, 1998; Li *et al.*, 2011). Many photospheric and coronal structures exhibit magnetic helicity ordered by hemisphere, with the northern (southern) hemisphere associated with left- (right-) handed helicity. In the heliosphere, magnetic clouds showing the same trends (Rust, 1994; Marubashi, 1997). Ulysses out-of-ecliptic observations of magnetic clouds over solar cycle 23 (Rees and Forsyth, 2003) further support the idea that ICMEs project the Hale cycle out into the heliosphere. These relations have important consequences for the means by which the solar cycle polarity reversal is communicated out to the heliospheric magnetic field, as discussed in Section 5.4.

Counterstreaming suprathermal electron observations of magnetic clouds indicate that approximately 50–60% of ICME-associated magnetic flux is formed of heliospheric loops with both ends attached to the Sun, with little change in this fraction between 1 and 5 AU (Gosling *et al.*, 1987; Shodhan *et al.*, 2000; Crooker *et al.*, 2004a; Riley *et al.*, 2004). Hence, Crooker *et al.* (2004a) and Riley *et al.* (2004) concluded that closed loops within ICMEs must add to the total open solar flux for long time scales (months to years). This is discussed further in Section 5.4.

### 4.3 Fine-scale structure

In addition to the large-scale, global features discussed thus far, single-point spacecraft observations reveal fluctuations in the HMF over all observable time scales. These are interpreted as a combination of spatial and temporal variations in the rest frame of the plasma, with waves, shocks, turbulence, tangential- and rotational discontinuities all likely contributing (e.g., Matthaeus *et al.*,

1986; Horbury *et al.*, 2001; Bruno *et al.*, 2001; Bruno and Carbone, 2013). A complete discussion of such phenomena is beyond the scope of this review, but we provide a brief overview of the observations which pertain to the origin of the HMF itself.

The solar wind exhibits a large array of different wave modes, many of which directly perturb the heliospheric magnetic field (see Tu and Marsch, 1995 and Marsch, 2006). The HMF in the high speed solar wind, particularly the polar regions at solar minimum, is dominated by Alfvénic fluctuations, flowing predominantly anti-sunward in the plasma frame (Smith *et al.*, 1995; Goldstein *et al.*, 1995; Horbury *et al.*, 1995). The solar wind is also highly turbulent, further adding to the spectrum of fluctuations in the HMF (Bruno and Carbone, 2013, and references therein). However, the full extent of this turbulence is debated, as magnetic field discontinuities could equally be the result of spacecraft encountering structures convected by the solar wind (Mariani *et al.*, 1973; Tu and Marsch, 1993; Bruno *et al.*, 2001; Borovsky, 2008). In this model of the HMF, the largest changes in the magnetic field direction are the result of crossing boundaries between large, coherent flux tubes, while the smaller fluctuations are true turbulent fluctuations within the flux tubes themselves. Such structures pass spacecraft with a time scale  $\sim 10$  minutes, thus the inferred flux tube size is in approximate agreement with super-granules on the Sun (Neugebauer *et al.*, 1995). However, the weak association between large magnetic discontinuities and compositional changes (Owens *et al.*, 2011b), mean they are equally likely to have formed by turbulence during transit, as be of solar origin.

The turbulent/filamentary nature of the HMF is important as it can place constraints on the solar wind formation mechanism. Figure 12 shows sketches of possible mechanisms for coronal heating, along with the implications for heliospheric magnetic field discontinuities (Cranmer, 2008). On the left, the corona is heated by reconnection between open solar flux and closed loops emerging through the photosphere (e.g., Fisk, 2003; Schwadron and McComas, 2003; Schwadron *et al.*, 2006) and the heliospheric magnetic field will naturally become tangled due to foot point motions. On the right, the corona is heated by waves and/or turbulence (e.g., Cranmer and van Ballegooijen, 2005; Verdini and Velli, 2007). The heliospheric magnetic field can then become tangled by turbulent motions, either propagating directly from the corona or generated in transit. Of course, it may be possible that both mechanisms are at play.

The largest amplitude waves, driven by fast ICMEs or the interaction of fast and slow solar wind streams, can steepen into interplanetary shock waves (Balogh *et al.*, 1995). CIR shocks and associated structures are discussed in Section 2.5. For fast ICMEs, shocks can form inside the corona. The region of compressed solar wind bounded by the shock and the ICME leading edge is referred to as the “sheath,” and is analogous to the planetary magnetosheaths (though see Siscoe and Odstrčil, 2008; Savani *et al.*, 2011). Magnetic fields in ICME sheaths can frequently be strong enough to trigger geomagnetic activity in their own right (Owens *et al.*, 2005), with a quarter (Richardson *et al.*, 2001) to a half (Tsurutani *et al.*, 1988) of all geomagnetic storms potentially attributable to ICME sheaths. As with CIRs, pre-existing structures or fluctuations in the upstream solar wind are swept up into the ICME sheath and compressed into planes perpendicular to the ICME leading edge or stream interface (Jones *et al.*, 2002).

Large magnetic field discontinuities in the solar wind would seem to provide ideal conditions for magnetic reconnection. The relatively high plasma beta, however, argues against widespread reconnection in the solar wind. This debate was finally settled in 2005, when signatures of reconnection, in the form of large-scale reconnection outflow exhausts, were observed in the near-Earth solar wind (Gosling *et al.*, 2005; Phan *et al.*, 2006). The leading edge of fast ICMEs seems to be a preferential location for reconnection, but it is also regularly occurs at low HMF shear angles in low plasma beta fields, often found within ICMEs (e.g., Gosling *et al.*, 2007).

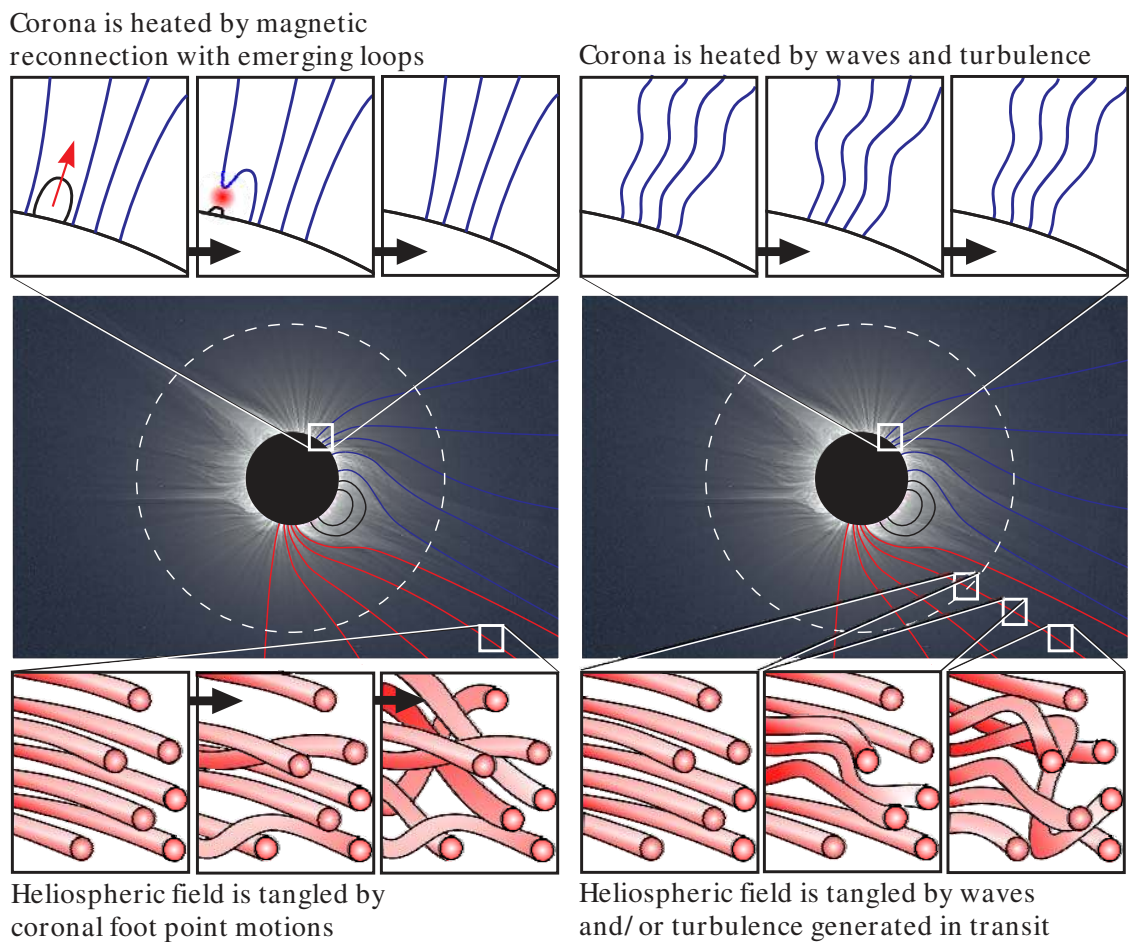


**Figure 12:** Sketches of proposed mechanisms for coronal heating and subsequent HMF braiding. On the left, the corona is heated by reconnection between open solar flux and closed loops emerging through the photosphere. In this model, the heliospheric magnetic field is likely to become tangled due to foot point motions. In the right-hand sketch, the corona is heated by waves or turbulence. The heliospheric magnetic field can then become tangled by turbulent motions, either propagating directly from the corona or generated in transit. Image reproduced by permission from Owens *et al.* (2011b), copyright by Springer.

## 5 Solar Cycle Variations

### 5.1 Solar minimum and the rise/declining phases

As discussed in Section 2.4, the HMF at solar minimum is well approximated by a dipolar-like magnetic field with a small inclination between the magnetic and rotational axes. Consequently, the heliospheric current sheet lies close to the rotational equator, perhaps still with some small warps due to weak non-dipolar structure. Coronal holes are confined to the polar regions while helmet streamers overlie the equator, thus fast solar wind fills the high-latitude heliosphere and the ecliptic plane generally sees alternate fast and slow solar wind streams. At this time, CMEs are much less frequent and are mainly observed at low latitudes (St Cyr *et al.*, 2000). In near-Earth space, the Parker spiral field is a very good approximation to the observed HMF, with relatively few ICMEs and, hence, few significant meridional excursions of the HMF.

As the solar cycle progresses, the complexity of the coronal magnetic field increases, with closed magnetic structures associated with streamers being found at increasingly high latitudes, allowing the HCS to extend to higher latitudes. This can also be interpreted as the underlying magnetic dipole field making a weaker contribution and becoming increasingly inclined to the rotational axis. Figure 13 shows the latitudinal extent of the HCS from PFSS extrapolations of the photospheric magnetic field and in situ observations from the Ulysses spacecraft. There is a strong solar cycle variation, from low latitudes at solar minimum, to all latitudes at solar maximum (e.g., Hoeksema *et al.*, 1983; Riley *et al.*, 2002).

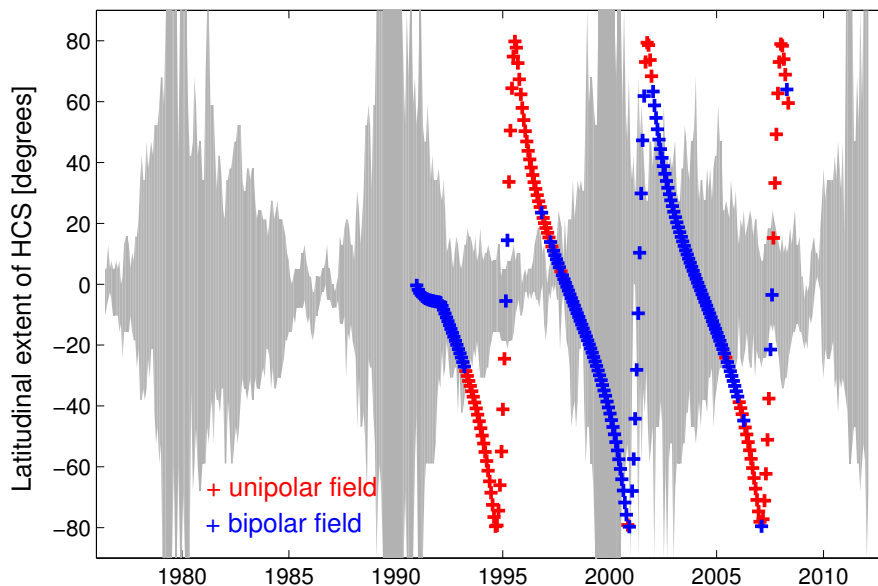


**Figure 13:** The location of the heliospheric current sheet as a function of solar cycle. The grey shaded area shows the latitudinal extent of the HCS estimated by a potential-field source-surface solution to the observed photospheric magnetic field. There is a strong solar cycle variation. Over plotted in red (blue) are the latitudes at which Ulysses encountered unipolar (bipolar) magnetic fields for whole Carrington rotations. Unipolar fields are expected polewards of the HCS, thus the Ulysses observations agree well with the PFSS reconstructions.

Associated with the HCS latitudinal extent increase, the coronal magnetic field structure begins to evolve more rapidly. CMEs become more frequent and cover a greater latitudinal span (e.g., [St Cyr \*et al.\*, 2000](#); [Yashiro \*et al.\*, 2004](#)). At greater number of ICMEs are encountered in the ecliptic, meaning the HMF, on average, exhibits a greater departure from an ideal Parker spiral.

## 5.2 Solar maximum

If the solar magnetic field remained approximately dipolar throughout the solar cycle, [Figure 13](#) suggests that with increasing solar activity, the HCS and associated slow solar wind band should extend to higher latitudes, while fast solar wind from the magnetic poles should be increasingly encountered in the ecliptic plane. During the rise and particularly the declining phase of the solar cycle, this picture does hold to some extent. However, around solar maximum, additional factors also come into play.

Firstly, the solar magnetic field is at its most dynamic around solar maximum. The coronal magnetic field evolves rapidly, and disturbances due to CMEs become much more frequent as a consequence. In near-Earth space, a significant fraction of the solar wind can be attributed directly to ICMEs ([Cane and Richardson, 2003](#); [Owens and Crooker, 2006](#)). Furthermore, quadrupolar and higher order moments of the solar magnetic field become more significant (e.g., [Hoeksema, 1991](#); [Wang \*et al.\*, 2000b](#)). The increased complexity of the magnetic field structure means that while the total open solar flux increases, it occurs in smaller spatial concentrations, in particular there is a decline in polar coronal hole area and, hence, a reduction in the occurrence of fast solar wind. As can be seen in the Ulysses solar maximum fast-latitude scan ([Figure 4](#)), this results in slow solar wind becoming prevalent at all latitudes. Consequently, CIRs are rare close to solar maximum, and interplanetary shocks result primary from fast ICMEs at this time.

Around the time of solar maximum, the polarity of the polar fields reverse, though the north and south poles do not typically reverse simultaneously, often showing around 1-year delay ([Babcock, 1959](#)). This polarity reversal process, as seen in the heliosphere, is discussed in [Section 5.4](#).

## 5.3 The space age solar cycles

Spacecraft in near-Earth space provide a reasonably complete record of the heliospheric magnetic field since 1965. The OMNI dataset (e.g., [King and Papitashvili, 2005](#), see also NSSDC: <http://omniweb.gsfc.nasa.gov/>) collates the near-Earth solar wind measurements from numerous spacecraft, mostly recently IMP8, Wind and ACE. The white line in the top panel of [Figure 14](#) shows the 27-day average of the scalar magnetic field intensity,  $B$ , in near-Earth space. The red line shows a 1-year average. The black-shaded area is international sunspot number,  $R$ , scaled to fit the axis.

The bottom panel shows the 27-day averages of the total unsigned heliospheric flux threading the 1-AU sphere,  $\Phi_{1\text{AU}} = 4\pi \text{ AU}^2 |B_R(1 \text{ AU})|$ , using a 1-day modulus of 1-hour measurements of  $|B_R(1 \text{ AU})|$  ([Owens \*et al.\*, 2008a](#)). Extrapolation from a single-point measurement of  $B_R$  to a global measure of total unsigned heliospheric flux is possible because of the Ulysses result of the latitude invariance in  $B_R$  ([Smith and Balogh, 2003](#); [Lockwood \*et al.\*, 2004](#)). Interpreting  $\Phi_{1\text{AU}}$  in terms of the coronal source-surface open solar flux is not trivial: As the 1-AU  $B_R$ -averaging interval is increased, e.g., from 1 hour to 1 day, the estimate of  $\Phi_{1\text{AU}}$  will decrease as more in/out flux is canceled ([Lockwood and Owens, 2009](#)). A value of 1 day gives the best match between in situ and PFSS estimates of coronal source surface OSF ([Wang \*et al.\*, 2000a](#)). The choice of this averaging interval is equivalent to defining a minimum size for  $B_R$  structures at 1 AU which originate at the coronal source surface, as opposed to forming between the source surface and 1 AU by kinematic effects, waves, turbulence, inverted HMF intervals, etc. There are currently a number of different approaches to dealing with this issue ([Smith and Balogh, 2003](#); [Owens \*et al.\*, 2008a](#); [Lockwood](#)

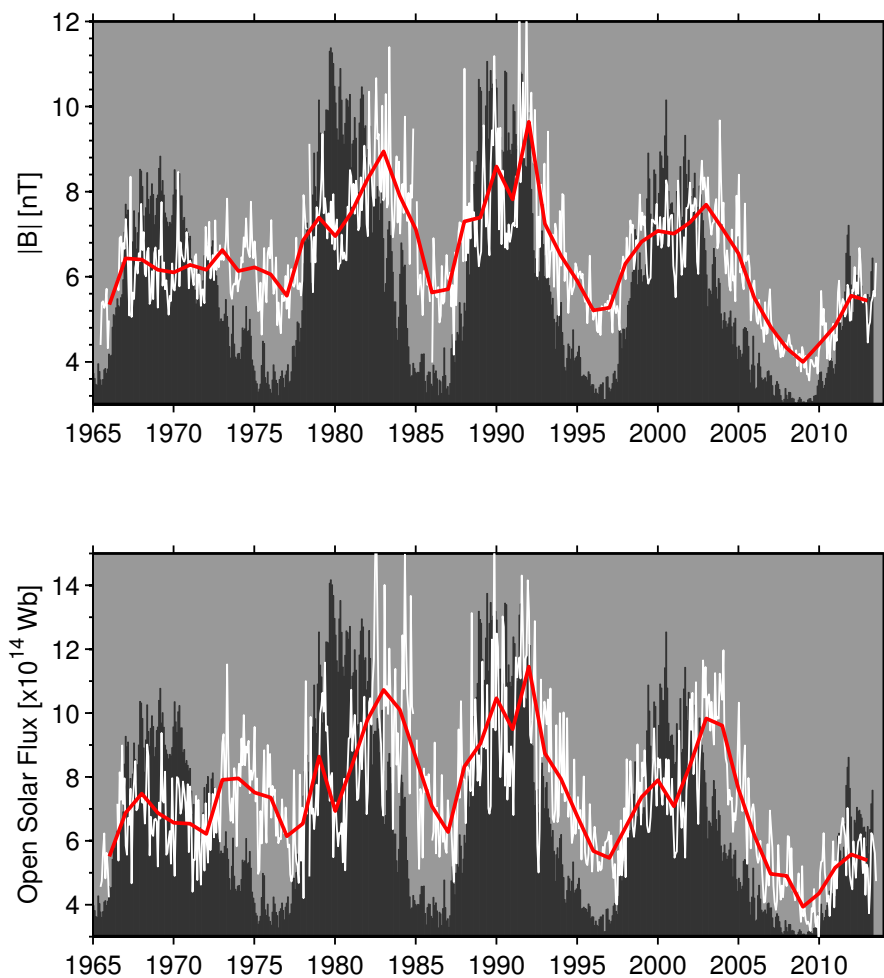


**Figure 14:** The heliospheric magnetic field during the space age. *Top:* Carrington-rotation averages (white) and annual averages (red) of the near-Earth HMF scalar magnetic field intensity from the OMNI dataset. The dark background shows the monthly sunspot number, scaled to fit the same axis. *Bottom:* Carrington-rotation (white) and 1-year (red) averages of 1-AU open solar flux, computed from the 1-day modulus of 1-hour measurements of the near-Earth radial magnetic field.

*et al.*, 2009a; Erdős and Balogh, 2012) which yield slightly different absolute values for the coronal source-surface OSF, but result in very similar solar cycle trends, discussed here.

Both  $|B|$  and  $\Phi_{1\text{AU}}$  show similar trends, with clear solar cycle variations in phase with the  $R$  variation (e.g., Slavin and Smith, 1983; Richardson *et al.*, 2000; Smith and Balogh, 2003; Owens *et al.*, 2008a; Zhou and Smith, 2009; Lockwood *et al.*, 2009a). However, the Gnevyshev gap, the small drop in solar magnetic activity at the time of solar maximum (Gnevyshev, 1977; Richardson *et al.*, 2002), is much more pronounced in  $\Phi$  and  $B$  than it is in sunspot number. While ICMEs are strongly associated with short-term enhancements in  $B$  and ICME rates are known to vary in phase with the solar cycle (Cane and Richardson, 2003; Riley *et al.*, 2006b), Richardson *et al.* (2000) concluded that the solar cycle variation in  $B$  was not a direct result of spacecraft being increasingly immersed in identifiable ICME material. See Section 5.4 for further discussion.

Cycle-to-cycle variations are discussed as part of long-term records of HMF in Section 5.5. However, we note here that the most recent solar minimum between the end of solar cycle 23 and the start of cycle 24, centred around 2008–2009, has been longest and deepest of the space age, with the lowest  $B$  and  $\Phi$  directly observed (Smith and Balogh, 2008; Lockwood *et al.*, 2009a,b). This has been accompanied by a significant reduction in the solar wind momentum flux (McComas *et al.*, 2008). At the photosphere, this minimum was manifest in the largest number of consecutive sunspot-free days since 1913 and the lowest polar magnetic field strength since routine observations began in 1975, which is likely the continuation of a decline in magnetic field strength which began several years previously (Wang *et al.*, 2009, see also the Wilcox Solar Observatory (WSO) long-term polar magnetic field observations). As of early 2013, the photospheric magnetic field suggests the North pole has changed polarity, while the southern polar field is slowly weakening prior to reversal (Shiota *et al.*, 2012). This suggests the Sun is presently very close to, if not just past, solar maximum, despite  $|B|$  and  $\Phi_{1\text{AU}}$  being at comparable levels to the 1996 solar minimum. Thus, cycle 24 is likely to be the weakest of the space age in terms of HMF strength and sunspot number (e.g., Svalgaard *et al.*, 2005). Section 5.5 puts these observations in a longer-term context.

## 5.4 Models of solar-cycle evolution

Over the solar cycle, the total unsigned OSF varies by approximately a factor two, roughly in phase with the sunspot variation. The large-scale solar polarity reversal means the structure of the heliospheric field varies from approximately a rotationally-aligned dipolar-like field at solar minimum, through increasing inclination and warping of the heliospheric current sheet towards solar maximum, before a return to rotationally-aligned dipolar field of opposite polarity the following minimum (Section 2.4). A number of theoretical constraints can be placed on the mechanism(s) by which this heliospheric evolution takes place. As the solar wind is super Alfvénic, the total OSF can only be increased by transporting a closed coronal loop out past the source surface so that it is dragged out into the heliosphere. As magnetic flux can not be transported back towards the Sun through the source surface, the only way to reduce the total OSF is by “disconnecting” open flux by magnetic reconfiguration below the source surface (though these open field lines may form closed loops in the heliosphere, so that flux is not truly disconnected from the Sun). There does, however, remain some debate about the magnetic flux systems and topologies involved in HMF creation and loss, and whether this process occurs in quasi-steady state or as a series of transient events.

The solar cycle evolution of photospheric magnetic flux has been well characterised by three complete cycles of observation (Schrijver and DeRosa, 2003; Hathaway, 2010). As predicted by Babcock (1959, 1961), existing polar fields are “eroded” by opposite polarity flux within emerging bipoles, such as sunspots, before being repopulated by flux of the opposite polarity. Wang and Sheeley Jr (2003) used a series of PFSS solutions to show that emerging mid-latitude bipoles cause pre-existing closed coronal loops to rise and destroy/create open flux. This process both increases

the total open solar flux, and creates/destroys open flux in the manner required for the polarity reversal. Over the solar cycle, the rise to solar maximum sees the axial dipole component of the Sun's field weaken, while the quadrupolar component strengthens, as observed (Hoeksema, 1991; Wang *et al.*, 2000a). While the polar fields are expected to reverse polarity around solar maximum, this model does not explicitly require the poles to flip simultaneously.

However, despite the success of such quasi-steady state models in capturing the large-scale evolution of the HMF, it is important to remember that PFSS models do not contain any time evolution and cannot account for transient structures such as CMEs. The location of newly opening solar magnetic flux between successive PFSS solutions correlates well with the timing and location of CMEs observed by coronagraphs (Luhmann *et al.*, 1998, 1999; Yeates *et al.*, 2010). Thus, in this “dynamic” picture, emerging active regions do not directly open new magnetic flux themselves, but act as source regions for CMEs, which provide the mechanism by which new magnetic loops are added to the heliosphere (see also Low, 2001). Indeed, in situ suprathermal electron observations clearly indicate that ICMEs carry new magnetic flux into the heliosphere (Gosling *et al.*, 1987, see also Section 3.1). The remaining question is the relative contribution to new HMF from CMEs compared with that from rising ambient loops. Coronagraph estimates of CME rates (St Cyr *et al.*, 2000; Yashiro *et al.*, 2004) coupled with in situ estimates of typical ICME magnetic flux content (Lynch *et al.*, 2005; Owens, 2008) suggest that CMEs potentially carry sufficient closed magnetic flux to account for the solar cycle variation of the OSF (Owens and Crooker, 2006, 2007; Connick *et al.*, 2011). Similarly, CMEs may act as important sinks of newly emerging magnetic helicity, by bodily removing it from the corona (Low, 2001; Lynch *et al.*, 2005). CMEs also project the Hale cycle of sunspot polarities out into the heliosphere. Gopalswamy *et al.* (2003) noted a correspondence between the cessation of high latitude CMEs and the polar field reversal. Low (2001); Low and Zhang (2004) suggested that CMEs play the role of emerging loops in the model of Wang and Sheeley Jr (2003), bodily removing old open solar flux from the corona for replacement by new open flux of opposite polarity, thus bringing about the global polarity reversal. More recently, Owens *et al.* (2007) suggested that the addition and removal of CME loops provides open flux transport, rather than open flux destruction, which agrees with suprathermal electron observations (McComas *et al.*, 1992; Pagel *et al.*, 2005), particularly within magnetic clouds (Crooker *et al.*, 2008; Lavraud *et al.*, 2011, see also Section 4.2.1).

In the Fisk model of coronal evolution, described in section 4.1, the solar cycle reversal of the HMF polarity can proceed as a rotation of the HCS (Fisk *et al.*, 1999), as suggested by Ulysses observations of the magnetic sector structure throughout the solar cycle (Jones *et al.*, 2003). Such a rotation would require “preferential” longitudes for the dipole axis as it approaches the solar equator, which have been suggested from observations of the HMF polarity (Neugebauer *et al.*, 2000). Fisk and Schwadron (2001) suggest HCS rotation is driven by a diffusive process involving reconnection between open and closed flux (interchange reconnection, Crooker *et al.*, 2002), which is thought to continually operate at the coronal hole boundaries (Nash *et al.*, 1988; Wang and Sheeley Jr, 2004). Unlike the potential-field corona, where open flux is confined to the interiors of coronal holes, this allows the foot points of the HMF to move through the streamer belt by reconnection with, and subsequent opening of, closed coronal loops. This could provide the mechanism for the release of the slow solar wind (Fisk and Schwadron, 2001) and explain the difference in first ionisation potential (FIP, Geiss *et al.*, 1995) between fast and slow streams (Zurbuchen *et al.*, 1998; Schwadron *et al.*, 1999), which is not accounted for by steady state models. However, there are theoretical issues with open solar flux existing within closed field regions (Antiochos *et al.*, 2007) and the MHD-simulated coronal response to evolving photospheric magnetic flux shows limited evidence of this behaviour (Lionello *et al.*, 2006; Linker *et al.*, 2011).



## 5.5 Long-term evolution of the HMF

There are a number of sources of proxy data for the heliospheric magnetic field hundreds to thousands of years into the past, allowing insight into long-term solar variability. This section contains a very brief summary of the long-term evolution of the HMF.

### 5.5.1 Geomagnetic activity

Records of geomagnetic variations can be used to infer the near-Earth solar wind conditions, primarily magnetic sector structure (Svalgaard, 1972), the magnetic field intensity and solar wind speed (e.g., Lockwood *et al.*, 1999; Svalgaard and Cliver, 2005, 2010). A complete review of the methods and techniques is presented by Lockwood (2013), but we note here that annual averages are typically estimated in order to avoid effects of the inclination of the ecliptic and terrestrial dipole relative to the solar rotation axis, and that the uncertainty in the solar wind reconstructions increases prior to  $\sim 1880$  as the number and quality of geomagnetic station records decreases significantly. For the 20th century, however, there is good agreement in HMF reconstructions from different geomagnetic records (Lockwood and Owens, 2011). Figure 15 shows the Lockwood *et al.* (2013a,b) (white) and Svalgaard and Cliver (2010) (yellow) reconstructions of near-Earth heliospheric magnetic field intensity,  $B$  (top). This has been converted to total unsigned OSF using the observationally constrained non-linear relation between  $B$  and OSF (Lockwood and Owens, 2011). OMNI spacecraft observations are shown in red and scaled sunspot number as dark background. The solar cycle variation is immediately obvious, but there is also a clear long-term variation, with the total OSF rising by nearly a factor 2 through the first half of the 20th century (Lockwood *et al.*, 1999).

### 5.5.2 Sunspot records

While there are issues with the intercalibration of sunspot records, the near-contiguous observations from 1610 to present (e.g., Hoyt and Schatten, 1998) are invaluable for understanding the evolution of the solar magnetic field. While the geomagnetic and cosmogenic isotope proxies relate directly to the HMF, sunspot records are related to large-scale magnetic features on the photosphere. In order to relate the two data sets, Solanki *et al.* (2000) proposed a continuity model of the OSF. The OSF source term must describe the rate at which new closed loops are added to the heliosphere and, thus, can be approximated by sunspot number. The loss term is more difficult to quantify. One approach is to assume various OSF contributions decay with different timescales (Krivova *et al.*, 2007; Vieira and Solanki, 2010). Owens and Lockwood (2012) instead assume that the OSF source term follows the CME rate, which is linked to the sunspot number (Webb and Howard, 1994), and that the OSF loss term follows the HCS tilt, owing to reconnection driven by differential rotation (Owens *et al.*, 2011a).

The green line in Figure 16 shows a reconstruction of total OSF based upon group sunspot number records (Owens and Lockwood, 2012). Obviously, prominent features from the sunspot record, such as the Dalton minimum around 1800–1820 and the Maunder minimum around 1650–1710, are also present in HMF reconstructions (Owens *et al.*, 2012). General agreement with the geomagnetic reconstructions for the 20th century, shown in white, is good, with both showing a rise and fall in the total OSF.

### 5.5.3 Cosmogenic isotope records

Ground-based neutron monitor counts, a proxy for the galactic cosmic ray flux at the top of the Earth's atmosphere, show a strong solar cycle variation in anti-phase with sunspot number. At solar maximum, the increase in OSF, coupled with the increased latitudinal extent of the HCS/CIRs,

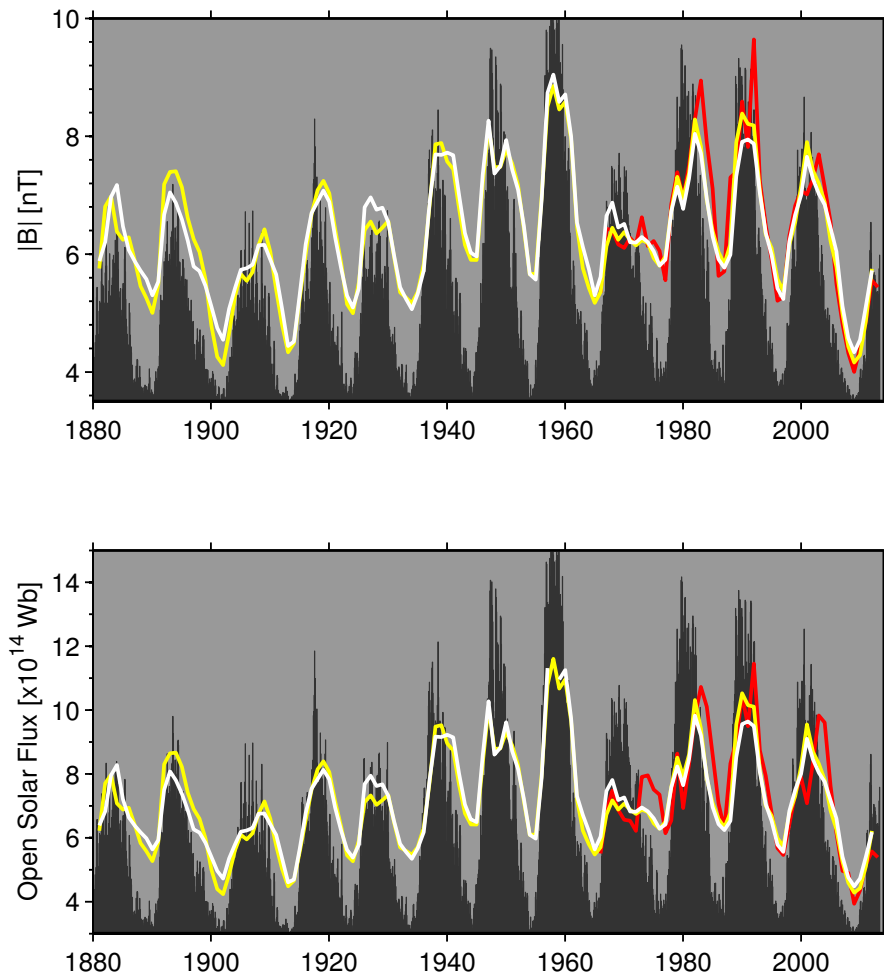


**Figure 15:** The heliospheric magnetic field over the last century. *Top:* The scalar magnetic field intensity,  $B$ . Spacecraft observations are shown in red, with reconstructions from geomagnetic activity data shown in white (Lockwood *et al.*, 2013a,b) and yellow (Svalgaard and Cliver, 2010). Sunspot number is shown as the dark background, scaled to fit the same axes. *Bottom:* 1-AU open solar flux (OSF), in the same format. Note that the geomagnetic reconstructions of  $B$  have been converted to OSF using an observationally constrained non-linear relation.

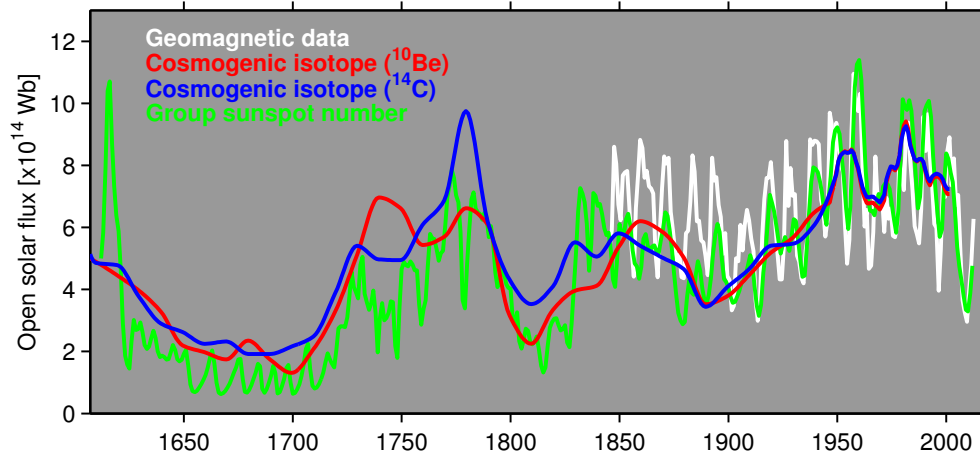


**Figure 16:** Reconstructions of the total OSF (bottom) from 1610 to present. White: The Lockwood *et al.* (2013a,b) geomagnetic reconstructions shown in Figure 15. Green: Group sunspot number-based reconstructions (see Owens and Lockwood, 2012, for more detail). Blue (red): Cosmogenic isotope reconstructions using  $^{14}\text{C}$  ( $^{10}\text{Be}$ ) (see Lockwood and Fröhlich, 2008, for more detail).

provides a more effective barrier to cosmic rays reaching the inner heliosphere (e.g., Usoskin *et al.*, 2005, and references therein). Cosmogenic isotope abundances, e.g., in ice-core records, can provide proxies for GCR flux and, hence, the HMF, over  $\sim 10\,000$  years (e.g., McCracken, 2007; Usoskin, 2013; Steinhilber *et al.*, 2010; Solanki *et al.*, 2004). The red and blue lines in Figure 16 show 22-year running averages of OSF inferred from heliospheric modulation potentials consistent with the  $^{10}\text{Be}$  and  $^{14}\text{C}$  abundances, respectively, since 1610 and extended to the space age using neutron monitor records (see Muscheler *et al.*, 2007; Lockwood and Fröhlich, 2008, and references therein for more detail). The long-term features such as the Dalton and Maunder minima, as well as the 20th century trends, are clearly present. The full record suggests that the HMF has been as strong as that of the space age on 24 previous occasions in the last 9300 years, though this grand solar maximum (GSM) is the longest in the record (Abreu *et al.*, 2008). Two of the 24 previous ends of GSMs have resulted in Maunder minimum-like conditions within 50 years (Barnard *et al.*, 2011).

## 6 Summary

This review has aimed to summarise our current understanding of the heliospheric magnetic field (HMF); its structure, its relation to the coronal and photospheric magnetic fields, its evolution over the solar cycle and longer periods. While some of this material, such as the Parker spiral, is mature and established enough to part of standard textbooks on space physics, other areas are very much developing at the time of writing. A number of HMF reviews already exist, so we have tried to focus on aspects of the heliospheric magnetic field where our knowledge is rapidly evolving: The outer heliosphere, the solar cycle variations, the link to solar wind formation, long-term variations in the HMF, etc. These areas will doubtless develop considerably over the coming months and years and this Living Review will be updated accordingly.

## Acknowledgements

We are indebted to two excellent anonymous referees who provided much useful input on the review. We are grateful to the Space Physics Data Facility (SPDF) and National Space Science Data Center (NSSDC) for OMNI data, as well as magnetic field data from Pioneer 6 and 7 (PI N. Ness), Pioneer 10 and 11 (PI E. Smith), Pioneer Venus Orbiter (PI C. Russell), Helios (PI N. Ness), Voyager (PI L. Burlaga) ICE/ISEE3 (PI E. Smith), Ulysses (PI A. Balogh) and STEREO (PI M. Acuña). We have also benefitted from the availability of WSO magnetograms (T. Hoeksema and Stanford University) Ulysses SWOOPS data (PI: D. McComas). The potential-field source-surface model used in this paper was based on code provided by J. Luhmann.

## References

- Abramenko, V., Yurchyshyn, V., Linker, J., Mikić, Z., Luhmann, J. and Lee, C.O., 2010, “Low-Latitude Coronal Holes at the Minimum of the 23rd Solar Cycle”, *Astrophys. J.*, **712**, 813–818. [DOI], [ADS], [arXiv:1002.1685 [astro-ph.SR]] (Cited on page 7.)
- Abreu, J.A., Beer, J., Steinhilber, F., Tobias, S.M. and Weiss, N.O., 2008, “For how long will the current grand maximum of solar activity persist?”, *Geophys. Res. Lett.*, **35**, L20109. [DOI], [ADS] (Cited on page 35.)
- Acuña, M.H., Curtis, D., Scheifele, J.L., Russell, C.T., Schroeder, P., Szabo, A. and Luhmann, J.G., 2008, “The STEREO/IMPACT Magnetic Field Experiment”, *Space Sci. Rev.*, **136**, 203–226. [DOI], [ADS] (Cited on page 5.)
- Alanko-Huotari, K., Usoskin, I.G., Mursula, K. and Kovaltsov, G.A., 2007, “Cyclic variations of the heliospheric tilt angle and cosmic ray modulation”, *Adv. Space Res.*, **40**, 1064–1069. [DOI], [ADS] (Cited on page 20.)
- Altschuler, M.D. and Newkirk Jr, G., 1969, “Magnetic Fields and the Structure of the Solar Corona. I: Methods of Calculating Coronal Fields”, *Solar Phys.*, **9**, 131–149. [DOI], [ADS] (Cited on page 7.)
- Antiochos, S.K., DeVore, C.R., Karpen, J.T. and Mikić, Z., 2007, “Structure and Dynamics of the Sun’s Open Magnetic Field”, *Astrophys. J.*, **671**, 936–946. [DOI], [ADS], [arXiv:0705.4430] (Cited on page 32.)
- Arge, C.N., Hildner, E., Pizzo, V.J. and Harvey, J.W., 2002, “Two solar cycles of nonincreasing magnetic flux”, *J. Geophys. Res.*, **107**, 1319. [DOI], [ADS] (Cited on page 6.)
- Babcock, H.D., 1959, “The Sun’s Polar Magnetic Field”, *Astrophys. J.*, **130**, 364–367. [DOI], [ADS] (Cited on pages 29 and 31.)
- Babcock, H.W., 1961, “The topology of the Sun’s magnetic field and the 22-year cycle”, *Astrophys. J.*, **133**, 527–587. [DOI], [ADS] (Cited on page 31.)
- Balogh, A. and Erdős, G., 2013, “The Heliospheric Magnetic Field”, *Space Sci. Rev.*, **176**, 177–215. [DOI], [ADS] (Cited on page 5.)
- Balogh, A. and Jokipii, J.R., 2009, “The Heliospheric Magnetic Field and Its Extension to the Inner Heliosheath”, *Space Sci. Rev.*, **143**, 85–110. [DOI], [ADS] (Cited on page 17.)
- Balogh, A., Beek, T.J., Forsyth, R.J., Hedgecock, P.C., Marquedant, R.J., Smith, E.J., Southwood, D.J. and Tsurutani, B.T., 1992, “The magnetic field investigation on the ULYSSES mission: Instrumentation and preliminary scientific results”, *Astron. Astrophys. Suppl.*, **92**, 221–236. [ADS] (Cited on page 5.)
- Balogh, A., Gonzalez-Esparza, J.A., Forsyth, R.J., Burton, M.E., Goldstein, B.E., Smith, E.J. and Bame, S.J., 1995, “Interplanetary shock waves: Ulysses observations in and out of the ecliptic plane”, *Space Sci. Rev.*, **72**, 171–180. [DOI], [ADS] (Cited on page 26.)
- Barnard, L., Lockwood, M., Hapgood, M.A., Owens, M.J., Davis, C.J. and Steinhilber, F., 2011, “Predicting space climate change”, *Geophys. Res. Lett.*, **38**, L16103. [DOI], [ADS] (Cited on page 35.)
- Behannon, K.W., Acuña, M.H., Burlaga, L.F., Lepping, R.P., Ness, N.F. and Neubauer, F.M., 1977, “Magnetic field experiment for Voyagers 1 and 2”, *Space Sci. Rev.*, **21**, 235–257. [DOI], [ADS] (Cited on page 5.)
- Belcher, J.W. and Davis Jr, L., 1971, “Large-Amplitude Alfvén Waves in the Interplanetary Medium, 2”, *J. Geophys. Res.*, **76**, 3534–3563. [DOI], [ADS] (Cited on page 17.)
- Bird, M.K. and Edenhofer, P., 1990, “Remote Sensing Observations of the Solar Corona”, in *Physics of the Inner Heliosphere, Vol. I: Large-Scale Phenomena*, (Eds.) Schwenn, R., Marsch, E., Physics and Chemistry in Space, 20, chap. 2, pp. 13–62, Springer, Berlin; New York. [DOI], [ADS] (Cited on page 22.)

- Borovsky, J.E., 2008, “Flux tube texture of the solar wind: Strands of the magnetic carpet at 1 AU?”, *J. Geophys. Res.*, **113**(A12), A08110. [DOI], [ADS] (Cited on page 26.)
- Borovsky, J.E., 2010, “On the variations of the solar wind magnetic field about the Parker spiral direction”, *J. Geophys. Res.*, **115**(A14), A09101. [DOI], [ADS] (Cited on page 9.)
- Bothmer, V. and Rust, D.M., 1997, “The field configuration of magnetic clouds and the solar cycle”, in *Coronal Mass Ejections*, (Eds.) Crooker, N., Joselyn, J.A., Feynman, J., Geophysical Monograph, 99, pp. 139–146, American Geophysical Union, Washington, DC. [DOI], [ADS] (Cited on page 25.)
- Bothmer, V. and Schwenn, R., 1998, “The structure and origin of magnetic clouds in the solar wind”, *Ann. Geophys.*, **16**, 1–24. [DOI], [ADS] (Cited on page 25.)
- Bruno, R. and Bavassano, B., 1997, “On the winding of the IMF spiral for slow and fast wind within the inner heliosphere”, *J. Geophys. Res.*, **24**, 2267–2270. [DOI], [ADS] (Cited on page 10.)
- Bruno, R. and Carbone, V., 2013, “The Solar Wind as a Turbulence Laboratory”, *Living Rev. Solar Phys.*, **10**, lrsp-2013-2. [DOI], [ADS]. URL (accessed 13 August 2013): <http://www.livingreviews.org/lrsp-2013-2> (Cited on page 26.)
- Bruno, R., Carbone, V., Veltri, P., Pietropaolo, E. and Bavassano, B., 2001, “Identifying intermittency events in the solar wind”, *Planet. Space Sci.*, **49**, 1201–1210. [DOI], [ADS] (Cited on page 26.)
- Burlaga, L.F., 1988, “Magnetic clouds and force-free fields with constant alpha”, *J. Geophys. Res.*, **93**, 7217–7224. [DOI], [ADS] (Cited on page 23.)
- Burlaga, L.F. and Ness, N.F., 1993, “Large-scale distant heliospheric magnetic field: Voyager 1 and 2 observations from 1986 through 1989”, *J. Geophys. Res.*, **98**, 17,451–17,460. [DOI], [ADS] (Cited on page 10.)
- Burlaga, L.F. and Richardson, J.D., 2000, “North-south flows at 47 AU: A heliospheric vortex street?”, *J. Geophys. Res.*, **105**(A5), 10,501–10,507. [DOI], [ADS] (Cited on page 18.)
- Burlaga, L.F., Sittler, E., Mariani, F. and Schwenn, R., 1981, “Magnetic loop behind an interplanetary shock: Voyager, Helios, and IMP 8 observations”, *J. Geophys. Res.*, **86**, 6673–6684. [DOI], [ADS] (Cited on page 23.)
- Burlaga, L.F., Lepping, R.P., Behannon, K.W., Klein, L.W. and Neubauer, F.M., 1982, “Large-scale variations of the interplanetary magnetic field: Voyager 1 and 2 observations between 1–5 AU”, *J. Geophys. Res.*, **87**, 4345–4353. [DOI], [ADS] (Cited on page 10.)
- Burlaga, L.F., Ness, N.F., Wang, Y.-M. and Sheeley Jr, N.R., 2002, “Heliospheric magnetic field strength and polarity from 1 to 81 AU during the ascending phase of solar cycle 23”, *J. Geophys. Res.*, **107**, 1410. [DOI], [ADS] (Cited on page 17.)
- Burlaga, L.F., Wang, C., Richardson, J.D. and Ness, N.F., 2003, “Large-Scale Magnetic Field Fluctuations and Development of the 1999–2000 Global Merged Interaction Region: 1–60 AU”, *Astrophys. J.*, **585**, 1158–1168. [DOI], [ADS] (Cited on page 18.)
- Cane, H.V. and Richardson, I.G., 2003, “Interplanetary coronal mass ejections in the near-Earth solar wind during 1996–2002”, *J. Geophys. Res.*, **108**, 1156. [DOI], [ADS] (Cited on pages 23, 24, 29, and 31.)
- Cargill, P.J., 2004, “On the Aerodynamic Drag Force Acting on Interplanetary Coronal Mass Ejections”, *Solar Phys.*, **221**, 135–149. [DOI], [ADS] (Cited on page 23.)
- Chenette, D.L., 1980, “The propagation of Jovian electrons to earth”, *J. Geophys. Res.*, **85**, 2243–2256. [DOI], [ADS] (Cited on page 20.)

- Chenette, D.L., Conlon, T.F. and Simpson, J.A., 1974, “Bursts of relativistic electrons from Jupiter observed in interplanetary space with the time variation of the planetary rotation period”, *J. Geophys. Res.*, **79**, 3551–3558. [DOI], [ADS] (Cited on page 20.)
- Chollet, E.E. and Giacalone, J., 2011, “Evidence of Confinement of Solar-energetic Particles to Interplanetary Magnetic Field Lines”, *Astrophys. J.*, **728**, 64. [DOI], [ADS] (Cited on page 20.)
- Clack, D., Forsyth, R.J. and Dunlop, M.W., 2000, “Ulysses observations of the magnetic field structure within CIRs”, *Geophys. Res. Lett.*, **27**, 625–628. [DOI], [ADS] (Cited on page 15.)
- Cliwer, E.W. and Ling, A.G., 2001, “22 Year Patterns in the Relationship of Sunspot Number and Tilt Angle to Cosmic-Ray Intensity”, *Astrophys. J. Lett.*, **551**, L189–L192. [DOI], [ADS] (Cited on page 20.)
- Coleman Jr, P.J., Davis Jr, L., Smith, E.J. and Sonett, C.P., 1962, “Interplanetary Magnetic Fields”, *Science*, **138**, 1099–1100. [DOI], [ADS] (Cited on page 9.)
- Connick, D.E., Smith, C.W. and Schwadron, N.A., 2011, “Interplanetary Magnetic Flux Depletion During Protracted Solar Minima”, *Astrophys. J.*, **727**, 8. [DOI], [ADS] (Cited on page 32.)
- Cranmer, S.R., 2008, “On Competing Models of Coronal Heating and Solar Wind Acceleration: The Debate in '08”, *arXiv*, e-print. [ADS], [arXiv:0804.3058] (Cited on pages 6 and 26.)
- Cranmer, S.R., 2009, “Coronal Holes”, *Living Rev. Solar Phys.*, **6**, lrsp-2009-3. [DOI], [ADS], [arXiv:0909.2847 [astro-ph.SR]]. URL (accessed 7 November 2013): <http://www.livingreviews.org/lrsp-2009-3> (Cited on page 7.)
- Cranmer, S.R. and van Ballegooijen, A.A., 2005, “On the Generation, Propagation, and Reflection of Alfvén Waves from the Solar Photosphere to the Distant Heliosphere”, *Astrophys. J. Suppl. Ser.*, **156**, 265–293. [DOI], [ADS], [astro-ph/0410639] (Cited on page 26.)
- Crooker, N.U., Gosling, J.T. and Kahler, S.W., 1998a, “Magnetic clouds at sector boundaries”, *J. Geophys. Res.*, **103**(A1), 301–306. [DOI], [ADS] (Cited on page 25.)
- Crooker, N.U., McAllister, A.H., Fitzenreiter, R.J. et al., 1998b, “Sector boundary transformation by an open magnetic cloud”, *J. Geophys. Res.*, **103**, 26,859–26,868. [DOI], [ADS] (Cited on page 25.)
- Crooker, N.U., Gosling, J.T., Bothmer, V. et al., 1999, “CIR Morphology, Turbulence, Discontinuities, and Energetic Particles”, *Space Sci. Rev.*, **89**, 179–220. [DOI], [ADS] (Cited on page 14.)
- Crooker, N.U., Gosling, J.T. and Kahler, S.W., 2002, “Reducing heliospheric flux from coronal mass ejections without disconnection”, *J. Geophys. Res.*, **107**(A2), 1028. [DOI], [ADS] (Cited on pages 22 and 32.)
- Crooker, N.U., Forsyth, R., Rees, A., Gosling, J.T. and Kahler, S.W., 2004a, “Counterstreaming electrons in magnetic clouds near 5 AU”, *J. Geophys. Res.*, **109**, A06110. [DOI], [ADS] (Cited on page 25.)
- Crooker, N.U., Kahler, S.W., Larson, D.E. and Lin, R.P., 2004b, “Large-scale magnetic field inversions at sector boundaries”, *J. Geophys. Res.*, **109**, A03108. [DOI], [ADS] (Cited on pages 19 and 22.)
- Crooker, N.U., Kahler, S.W., Gosling, J.T. and Lepping, R.P., 2008, “Evidence in magnetic clouds for systematic open flux transport on the Sun”, *J. Geophys. Res.*, **113**(A12), A12107. [DOI], [ADS] (Cited on page 32.)
- Davis, C.J., Davies, J.A., Lockwood, M., Rouillard, A.P., Eyles, C.J. and Harrison, R.A., 2009, “Stereoscopic imaging of an Earth-impacting solar coronal mass ejection: A major milestone for the STEREO mission”, *Geophys. Res. Lett.*, **36**, L08102. [DOI], [ADS] (Cited on page 23.)
- Davis Jr, L., Smith, E.J., Coleman Jr, P.J. and Sonett, C.P., 1966, “Interplanetary Magnetic Measurements”, in *The Solar Wind*, Proceedings of a conference held at the California Institute of Technology, Pasadena, 1–4 April, 1964, (Eds.) Mackin Jr, R.J., Neugebauer, M., JPL Technical Report, 32-630, Pergamon Press; JPL, Oxford; New York; Pasadena. [ADS] (Cited on page 9.)

- Erdős, G. and Balogh, A., 2010, “North-south asymmetry of the location of the heliospheric current sheet revisited”, *J. Geophys. Res.*, **115**, A01105. [DOI], [ADS] (Cited on page 23.)
- Erdős, G. and Balogh, A., 2012, “Magnetic Flux Density Measured in Fast and Slow Solar Wind Streams”, *Astrophys. J.*, **753**, 130. [DOI], [ADS] (Cited on page 31.)
- Feldman, W.C., Asbridge, J.R., Bame, S.J., Montgomery, M.D. and Gary, S.P., 1975, “Solar wind electrons”, *J. Geophys. Res.*, **80**, 4181–4196. [DOI], [ADS] (Cited on page 19.)
- Ferreira, S.E. and Potgieter, M.S., 2003, “Modulation over a 22-year cosmic ray cycle: On the tilt angles of the heliospheric current sheet”, *Adv. Space Res.*, **32**, 657–662. [DOI], [ADS] (Cited on page 20.)
- Fisk, L.A., 1996, “Motion of the footpoints of heliospheric magnetic field lines at the Sun: Implications for recurrent energetic particle events at high heliographic latitudes”, *J. Geophys. Res.*, **101**, 15,547–15,554. [DOI], [ADS] (Cited on pages 20 and 22.)
- Fisk, L.A., 2003, “Acceleration of the solar wind as a result of the reconnection of open magnetic flux with coronal loops”, *J. Geophys. Res.*, **108**, 1157. [DOI], [ADS] (Cited on pages 22 and 26.)
- Fisk, L.A. and Schwadron, N.A., 2001, “The Behavior of the Open Magnetic Field of the Sun”, *Astrophys. J.*, **560**, 425–438. [DOI], [ADS] (Cited on page 32.)
- Fisk, L.A., Zurbuchen, T.H. and Schwadron, N.A., 1999, “Coronal hole boundaries and their interaction with adjacent regions”, *Space Sci. Rev.*, **87**, 43–54. [DOI], [ADS] (Cited on pages 22 and 32.)
- Forsyth, R.J., Balogh, A. and Smith, E.J., 2002, “The underlying direction of the heliospheric magnetic field through the Ulysses first orbit”, *J. Geophys. Res.*, **107**, 1405. [DOI], [ADS] (Cited on pages 10 and 22.)
- Geiss, J., Gloeckler, G. and von Steiger, R., 1995, “Origin of the Solar Wind From Composition Data”, *Space Sci. Rev.*, **72**, 49–60. [DOI], [ADS] (Cited on page 32.)
- Gloeckler, G., Fisk, L.A., Hefti, S. et al., 1999, “Unusual composition of the solar wind in the 2-3 May 1998 CME observed with SWICS on ACE”, *Geophys. Res. Lett.*, **26**, 157–160. [DOI], [ADS] (Cited on page 23.)
- Gloeckler, G., Geiss, J. and Fisk, L.A., 2001, “Heliospheric and interstellar phenomena revealed from observations of pickup ions”, in *The Heliosphere Near Solar Minimum: The Ulysses perspective*, (Eds.) Balogh, A., Marsden, R.G., Smith, E.J., Springer–Praxis Books in Astrophysics and Astronomy, chap. 7, pp. 287–326, Springer; Praxis, Berlin; New York; Chichester. [ADS], [Google Books] (Cited on page 21.)
- Gnevyshev, M.N., 1977, “Essential features of the 11-year solar cycle”, *Solar Phys.*, **51**, 175–183. [DOI], [ADS] (Cited on page 31.)
- Goldstein, B.E., Smith, E.J., Balogh, A., Horbury, T.S., Goldstein, M.L. and Roberts, D.A., 1995, “Properties of magnetohydrodynamic turbulence in the solar wind as observed by Ulysses at high heliographic latitudes”, *Geophys. Res. Lett.*, **22**, 3393–3396. [DOI], [ADS] (Cited on page 26.)
- Gopalswamy, N., Lara, A., Lepping, R.P., Kaiser, M.L., Berdichevsky, D. and St Cyr, O.C., 2000, “Interplanetary acceleration of coronal mass ejections”, *Geophys. Res. Lett.*, **27**, 145–148. [DOI], [ADS] (Cited on page 23.)
- Gopalswamy, N., Lara, A., Yashiro, S. and Howard, R.A., 2003, “Coronal Mass Ejections and Solar Polarity Reversal”, *Astrophys. J. Lett.*, **598**, L63–L66. [DOI], [ADS] (Cited on page 32.)
- Gosling, J.T., 1990, “Coronal mass ejections and magnetic flux ropes in interplanetary space”, in *Physics of Magnetic Flux Ropes*, Based on papers presented at the AGU Chapman Conference, held in Hamilton, Bermuda on March 27–31, 1989, (Eds.) Russell, C.T., Priest, E.R., Lee, L.C., Geophysical Monograph, 58, pp. 343–364, American Geophysical Union, Washington, DC. [DOI], [ADS] (Cited on page 24.)



- Gosling, J.T., 1993, “The solar flare myth”, *J. Geophys. Res.*, **98**, 18,937–18,950. [DOI], [ADS] (Cited on pages 23 and 24.)
- Gosling, J.T. and Pizzo, V.J., 1999, “Formation and Evolution of Corotating Interaction Regions and their Three Dimensional Structure”, *Space Sci. Rev.*, **89**, 21–52. [DOI], [ADS] (Cited on pages 14 and 15.)
- Gosling, J.T., Baker, D.N., Bame, S.J., Feldman, W.C., Zwickl, R.D. and Smith, E.J., 1987, “Bidirectional solar wind electron heat flux events”, *J. Geophys. Res.*, **92**, 8519–8535. [DOI], [ADS] (Cited on pages 20, 25, and 32.)
- Gosling, J.T., Bame, S.J., Feldman, W.C., McComas, D.J., Phillips, J.L. and Goldstein, B.E., 1993a, “Counterstreaming suprathermal electron events upstream of corotating shocks in the solar wind beyond  $\sim 2$  AU: Ulysses”, *Geophys. Res. Lett.*, **20**, 2335–2338. [DOI], [ADS] (Cited on page 20.)
- Gosling, J.T., Bame, S.J., McComas, D.J., Phillips, J.L., Pizzo, V.J., Goldstein, B.E. and Neugebauer, M., 1993b, “Latitudinal variation of solar wind corotating stream interaction regions: Ulysses”, *Geophys. Res. Lett.*, **20**, 2789–2792. [DOI], [ADS] (Cited on page 15.)
- Gosling, J.T., Skoug, R.M. and Feldman, W.C., 2001, “Solar wind electron halo depletions at  $90^\circ$  pitch angle”, *Geophys. Res. Lett.*, **28**, 4155–4158. [DOI], [ADS] (Cited on page 20.)
- Gosling, J.T., Skoug, R.M., McComas, D.J. and Smith, C.W., 2005, “Magnetic disconnection from the Sun: Observations of a reconnection exhaust in the solar wind at the heliospheric current sheet”, *Geophys. Res. Lett.*, **32**, L05105. [DOI], [ADS] (Cited on page 26.)
- Gosling, J.T., Eriksson, S., McComas, D.J., Phan, T.D. and Skoug, R.M., 2007, “Multiple magnetic reconnection sites associated with a coronal mass ejection in the solar wind”, *J. Geophys. Res.*, **112**(A11), A08106. [DOI], [ADS] (Cited on page 26.)
- Gruntman, M., 1997, “Energetic neutral atom imaging of space plasmas”, *Rev. Sci. Instrum.*, **68**, 3617–3656. [DOI], [ADS] (Cited on page 21.)
- Gurnett, D.A., Kurth, W.S., Burlaga, L.F. and Ness, N.F., 2013, “In Situ Observations of Interstellar Plasma with Voyager 1”, *Science*, **341**, 1489–1492. [DOI] (Cited on page 17.)
- Hale, G.E. and Nicholson, S.B., 1925, “The Law of Sun-Spot Polarity”, *Astrophys. J.*, **62**, 270–300. [DOI], [ADS] (Cited on page 25.)
- Hammond, C.M., Feldman, W.C., McComas, D.J., Phillips, J.L. and Forsyth, R.J., 1996, “Variation of electron-strahl width in the high-speed solar wind: Ulysses observations”, *Astron. Astrophys.*, **316**, 350–354. [ADS] (Cited on page 20.)
- Hanlon, P.G., Dougherty, M.K., Forsyth, R.J., Owens, M.J., Hansen, K.C., Tóth, G., Crary, F.J. and Young, D.T., 2004, “On the evolution of the solar wind between 1 and 5 AU at the time of the Cassini Jupiter flyby: Multispacecraft observations of interplanetary coronal mass ejections including the formation of a merged interaction region”, *J. Geophys. Res.*, **109**, A09S03. [DOI], [ADS] (Cited on page 18.)
- Harrison, R.A., 1995, “The nature of solar flares associated with coronal mass ejection”, *Astron. Astrophys.*, **304**, 585–594. [ADS] (Cited on page 23.)
- Hathaway, D.H., 2010, “The Solar Cycle”, *Living Rev. Solar Phys.*, **7**, lrsp-2010-1. [DOI], [ADS]. URL (accessed 17 April 2013): <http://www.livingreviews.org/lrsp-2010-1> (Cited on page 31.)
- Hoeksema, J.T., 1991, “Large-scale solar and heliospheric magnetic fields”, *Adv. Space Res.*, **11**, 15–24. [DOI], [ADS] (Cited on pages 29 and 32.)
- Hoeksema, J.T. and Scherrer, P.H., 1986, “An atlas of photospheric magnetic field observations and computed coronal magnetic fields: 1976–1985”, *Solar Phys.*, **105**, 205–211. [DOI], [ADS] (Cited on page 6.)

- Hoeksema, J.T., Wilcox, J.M and Scherrer, P.H, 1982, “Structure of the heliospheric current sheet in the early portion of sunspot cycle 21”, *J. Geophys. Res.*, **87**(A12), 10,331–10,338. [DOI], [ADS] (Cited on pages 7 and 11.)
- Hoeksema, J.T., Wilcox, J.M. and Scherrer, P.H., 1983, “The structure of the heliospheric current sheet: 1978–1982”, *J. Geophys. Res.*, **88**(A12), 9910–9918. [DOI], [ADS] (Cited on page 28.)
- Horbury, T.S., Balogh, A., Forsyth, R.J. and Smith, E.J., 1995, “ULYSSES magnetic field observations of fluctuations within polar coronal flows”, *Ann. Geophys.*, **13**, 105–107. [ADS] (Cited on page 26.)
- Horbury, T.S., Burgess, D., Fränz, M. and Owen, C.J., 2001, “Three spacecraft observations of solar wind discontinuities”, *Geophys. Res. Lett.*, **28**, 677–680. [DOI], [ADS] (Cited on page 26.)
- Hoyt, D.V. and Schatten, K.H., 1998, “Group Sunspot Numbers: A New Solar Activity Reconstruction”, *Solar Phys.*, **181**, 491–512. [DOI], [ADS] (Cited on page 33.)
- Jacobs, C., Rousev, I.I., Lugaz, N. and Poedts, S., 2009, “The Internal Structure of Coronal Mass Ejections: Are all Regular Magnetic Clouds Flux Ropes?”, *Astrophys. J. Lett.*, **695**, L171–L175. [DOI] (Cited on page 24.)
- Jokipii, J.R., Levy, E.H. and Hubbard, W.B., 1977, “Effects of particle drift on cosmic-ray transport. I. General properties, application to solar modulation”, *Astrophys. J.*, **213**, 861–868. [DOI], [ADS] (Cited on page 20.)
- Jones, G.H., Rees, A., Balogh, A. and Forsyth, R.J., 2002, “The draping of heliospheric magnetic fields upstream of coronal mass ejecta”, *Geophys. Res. Lett.*, **29**, 1520. [DOI], [ADS] (Cited on pages 11, 23, and 26.)
- Jones, G.H., Balogh, A. and Smith, E.J., 2003, “Solar magnetic field reversal as seen at Ulysses”, *Geophys. Res. Lett.*, **30**, 8028. [DOI], [ADS] (Cited on pages 12 and 32.)
- Kahler, S.W., Crooker, N.U. and Gosling, J.T., 1996, “The topology of intrasector reversals of the interplanetary magnetic field”, *J. Geophys. Res.*, **101**, 24,373–24,382. [DOI], [ADS] (Cited on page 22.)
- Kahler, S.W., Haggerty, D.K. and Richardson, I.G., 2011, “Magnetic Field-line Lengths in Interplanetary Coronal Mass Ejections Inferred from Energetic Electron Events”, *Astrophys. J.*, **736**, 106. [DOI], [ADS] (Cited on page 20.)
- King, J.H. and Papitashvili, N.E., 2005, “Solar wind spatial scales in and comparisons of hourly Wind and ACE plasma and magnetic field data”, *J. Geophys. Res.*, **110**(A9), A02104. [DOI], [ADS] (Cited on page 29.)
- Klein, L.W. and Burlaga, L.F., 1982, “Interplanetary magnetic clouds at 1 AU”, *J. Geophys. Res.*, **87**, 613–624. [DOI], [ADS] (Cited on page 23.)
- Kóta, J. and Jokipii, J.R., 1995, “Corotating Variations of Cosmic Rays Near the South Heliospheric Pole”, *Science*, **268**, 1024–1025. [DOI], [ADS] (Cited on page 22.)
- Krimigis, S.M., Roelof, E.C., Decker, R.B. and Hill, M.E., 2011, “Zero outward flow velocity for plasma in a heliosheath transition layer”, *Nature*, **474**, 359–361. [DOI], [ADS] (Cited on page 17.)
- Krivova, N.A., Balmaceda, L. and Solanki, S.K., 2007, “Reconstruction of solar total irradiance since 1700 from the surface magnetic flux”, *Astron. Astrophys.*, **467**, 335–346. [DOI], [ADS] (Cited on page 33.)
- Larson, D.E., Lin, R.P., McTiernan, J.M. et al., 1997, “Tracing the topology of the October 18–20, 1995, magnetic cloud with  $\sim 0.1 - 10^2$  keV electrons”, *Geophys. Res. Lett.*, **24**, 1911–1914. [DOI], [ADS] (Cited on page 20.)

- Lavraud, B., Owens, M.J. and Rouillard, A.P., 2011, “In Situ Signatures of Interchange Reconnection between Magnetic Clouds and Open Magnetic Fields: A Mechanism for the Erosion of Polar Coronal Holes?”, *Solar Phys.*, **270**, 285–296. [DOI], [ADS] (Cited on page 32.)
- Lee, C.O., Luhmann, J.G., Hoeksema, J.T., Sun, X., Arge, C.N. and de Pater, I., 2011, “Coronal Field Opens at Lower Height During the Solar Cycles 22 and 23 Minimum Periods: IMF Comparison Suggests the Source Surface Should Be Lowered”, *Solar Phys.*, **269**, 367–388. [DOI], [ADS] (Cited on page 7.)
- Lepping, R.P., Jones, J.A. and Burlaga, L.F., 1990, “Magnetic Field Structure of Interplanetary Magnetic Clouds at 1 AU”, *J. Geophys. Res.*, **95**, 11,957–11,965. [DOI], [ADS] (Cited on page 23.)
- Lepri, S.T. and Zurbuchen, T.H., 2004, “Iron charge state distributions as an indicator of hot ICMEs: Possible sources and temporal and spatial variations during solar maximum”, *J. Geophys. Res.*, **109**, A01112. [DOI], [ADS] (Cited on page 23.)
- Levine, R.H., Altschuler, M.D. and Harvey, J.W., 1977, “Solar sources of the interplanetary magnetic field and solar wind”, *J. Geophys. Res.*, **82**, 1061–1065. [DOI], [ADS] (Cited on page 7.)
- Li, Y., Luhmann, J.G., Lynch, B.J. and Kilpua, E.K.J., 2011, “Cyclic Reversal of Magnetic Cloud Poloidal Field”, *Solar Phys.*, **270**, 331–346. [DOI], [ADS] (Cited on page 25.)
- Linker, J., Mikić, Z., Biesecker, D.A. et al., 1999, “Magnetohydrodynamic modeling of the solar corona during Whole Sun Month”, *J. Geophys. Res.*, **104**, 9809–9830. [DOI], [ADS] (Cited on page 7.)
- Linker, J.A., Mikić, Z., Lionello, R., Riley, P., Amari, T. and Odstrčil, D., 2003, “Flux cancellation and coronal mass ejections”, *Phys. Plasmas*, **10**, 1971–1978. [DOI] (Cited on page 7.)
- Linker, J.A., Lionello, R., Mikić, Z., Titov, V.S. and Antiochos, S.K., 2011, “The Evolution of Open Magnetic Flux Driven by Photospheric Dynamics”, *Astrophys. J.*, **731**, 110. [DOI], [ADS] (Cited on page 32.)
- Linsky, J.L., 2009, “Results from the ISSI Workshop: ‘From the Outer Heliosphere to the Local Bubble: Comparison of New Observations with Theory’”, in *The Local Bubble and Beyond II*, Proceedings of the International Conference, Philadelphia, PA, 21–24 April 2008, (Eds.) Smith, R.K., Snowden, S.L., Kuntz, K.D., AIP Conference Series, 1156, pp. 184–195, American Institute of Physics, Melville, NY. [DOI], [ADS] (Cited on page 17.)
- Linsky, J.L., Diplas, A., Wood, B.E., Brown, A., Ayres, T.R. and Savage, B.D., 1995, “Deuterium and the Local Interstellar Medium Properties for the Procyon and Capella Lines of Sight”, *Astrophys. J.*, **451**, 335–351. [DOI], [ADS] (Cited on page 17.)
- Lionello, R., Linker, J.A., Mikić, Z. and Riley, P., 2006, “The Latitudinal Excursion of Coronal Magnetic Field Lines in Response to Differential Rotation: MHD Simulations”, *Astrophys. J. Lett.*, **642**, L69–L72. [DOI], [ADS] (Cited on page 32.)
- Lockwood, M., 2013, “Reconstruction and Prediction of Variations in the Open Solar Magnetic Flux and Interplanetary Conditions”, *Living Rev. Solar Phys.*, **10**, lrsp-2013-4. [DOI], [ADS]. URL (accessed 7 November 2013): <http://www.livingreviews.org/lrsp-2013-4> (Cited on page 33.)
- Lockwood, M. and Fröhlich, C., 2008, “Recent oppositely directed trends in solar climate forcings and the global mean surface air temperature. II. Different reconstructions of the total solar irradiance variation and dependence on response time scale”, *Proc. R. Soc. London, Ser. A*, **464**, 1367–1385. [DOI], [ADS] (Cited on page 35.)
- Lockwood, M. and Owens, M., 2009, “The Accuracy of Using the Ulysses Result of the Spatial Invariance of the Radial Heliospheric Field to Compute the Open Solar Flux”, *Astrophys. J.*, **701**, 964–973. [DOI], [ADS] (Cited on page 29.)

- Lockwood, M. and Owens, M.J., 2011, “Centennial changes in the heliospheric magnetic field and open solar flux: The consensus view from geomagnetic data and cosmogenic isotopes and its implications”, *J. Geophys. Res.*, **116**, A04109. [DOI], [ADS] (Cited on page 33.)
- Lockwood, M., Stamper, R. and Wild, M.N., 1999, “A doubling of the Sun’s coronal magnetic field during the past 100 years”, *Nature*, **399**, 437–439. [DOI], [ADS] (Cited on page 33.)
- Lockwood, M., Forsyth, R.J., Balogh, A. and McComas, D.J., 2004, “Open solar flux estimates from near-Earth measurements of the interplanetary magnetic field: comparison of the first two perihelion passes of the Ulysses spacecraft”, *Ann. Geophys.*, **22**, 1395–1405. [DOI], [ADS] (Cited on pages 10 and 29.)
- Lockwood, M., Owens, M. and Rouillard, A.P., 2009a, “Excess open solar magnetic flux from satellite data: 2. A survey of kinematic effects”, *J. Geophys. Res.*, **114**(A13), A11104. [DOI], [ADS] (Cited on pages 29 and 31.)
- Lockwood, M., Rouillard, A.P. and Finch, I.D., 2009b, “The Rise and Fall of Open Solar Flux During the Current Grand Solar Maximum”, *Astrophys. J.*, **700**, 937–944. [DOI], [ADS] (Cited on page 31.)
- Lockwood, M., Barnard, L., Nevanlinna, H., Owens, M.J., Harrison, R.G., Rouillard, A.P. and Davis, C.J., 2013a, “Reconstruction of geomagnetic activity and near-Earth interplanetary conditions over the past 167 yr – Part 1: A new geomagnetic data composite”, *Ann. Geophys.*, **31**, 1957–1977. [DOI] (Cited on pages 33, 34, and 35.)
- Lockwood, M., Barnard, L., Nevanlinna, H., Owens, M.J., Harrison, R.G., Rouillard, A.P. and Davis, C.J., 2013b, “Reconstruction of geomagnetic activity and near-Earth interplanetary conditions over the past 167 yr – Part 2: A new reconstruction of the interplanetary magnetic field”, *Ann. Geophys.*, **31**, 1979–1992. [DOI] (Cited on pages 33, 34, and 35.)
- Low, B.C., 2001, “Coronal mass ejections, magnetic flux ropes, and solar magnetism”, *J. Geophys. Res.*, **106**, 25,141–25,160. [DOI], [ADS] (Cited on page 32.)
- Low, B.C. and Zhang, M., 2004, “Global Magnetic-Field Reversal in the Corona”, in *Solar Variability and its Effects on Climate*, (Eds.) Pap, J.M., Fox, P., Geophysical Monograph, 141, pp. 51–64, American Geophysical Union, Washington, DC. [DOI], [ADS] (Cited on page 32.)
- Luhmann, J.G., Gosling, J.T., Hoeksema, J.T. and Zhao, X., 1998, “The relationship between large-scale solar magnetic field evolution and coronal mass ejections”, *J. Geophys. Res.*, **103**, 6585–6594. [DOI], [ADS] (Cited on page 32.)
- Luhmann, J.G., Larson, D., Hoeksema, J.T., Zhao, X.-P., Arge, N. and St Cyr, O.C., 1999, “Connections between the slow solar wind, CMEs, and the helmet streamer belt inferred from coronal field models”, in *Solar Wind Nine*, Proceedings of the Ninth International Solar Wind Conference, Nantucket, MA, 5–9 October 1998, (Eds.) Habbal, S.R., Esser, R., Hollweg, J.V., Isenberg, P.A., AIP Conference Proceedings, 471, pp. 725–728, American Institute of Physics, Woodbury, NY. [DOI], [ADS] (Cited on page 32.)
- Luhmann, J.G., Lee, C.O., Li, Y. et al., 2009, “Solar Wind Sources in the Late Declining Phase of Cycle 23: Effects of the Weak Solar Polar Field on High Speed Streams”, *Solar Phys.*, **256**, 285–305. [DOI], [ADS] (Cited on page 7.)
- Lynch, B.J., Gruesbeck, J.R., Zurbuchen, T.H. and Antiochos, S.K., 2005, “Solar cycle dependent helicity transport by magnetic clouds”, *J. Geophys. Res.*, **110**, A08107. [DOI], [ADS] (Cited on pages 25 and 32.)
- Maksimovic, M., Zouganelis, I., Chaufray, J.-Y. et al., 2005, “Radial evolution of the electron distribution functions in the fast solar wind between 0.3 and 1.5 AU”, *J. Geophys. Res.*, **110**, A09104. [DOI], [ADS] (Cited on page 20.)

- Mariani, F., Bavassano, B., Villante, U. and Ness, N.F., 1973, “Variations of the occurrence rate of discontinuities in the interplanetary magnetic field”, *J. Geophys. Res.*, **78**, 8011–8022. [DOI], [ADS] (Cited on page 26.)
- Marsch, E., 2006, “Kinetic Physics of the Solar Corona and Solar Wind”, *Living Rev. Solar Phys.*, **3**, lrsp-2006-1. [DOI], [ADS]. URL (accessed 17 April 2013): <http://www.livingreviews.org/lrsp-2006-1> (Cited on page 26.)
- Marubashi, K., 1997, “Interplanetary Magnetic Flux Ropes and Solar Filaments”, in *Coronal Mass Ejections*, (Eds.) Crooker, N.U., Joselyn, J.A., Feynman, J., Geophysical Monograph, 99, pp. 147–156, American Geophysical Union, Washington, DC. [DOI] (Cited on page 25.)
- Matthaeus, W.H., Goldstein, M.L. and King, J.H., 1986, “An interplanetary magnetic field ensemble at 1 AU”, *J. Geophys. Res.*, **91**, 59–69. [DOI], [ADS] (Cited on page 25.)
- McComas, D.J. and Schwadron, N.A., 2006, “An explanation of the Voyager paradox: Particle acceleration at a blunt termination shock”, *Geophys. Res. Lett.*, **33**, L04102. [DOI], [ADS] (Cited on page 17.)
- McComas, D.J., Gosling, J.T., Phillips, J.L., Bame, S.J., Luhmann, J.G. and Smith, E.J., 1989, “Electron heat flux dropouts in the solar wind: Evidence for interplanetary magnetic field reconnection?”, *J. Geophys. Res.*, **94**, 6907–6916. [DOI], [ADS] (Cited on page 20.)
- McComas, D.J., Gosling, J.T. and Phillips, J.L., 1992, “Interplanetary magnetic flux: Measurement and balance”, *J. Geophys. Res.*, **97**, 171–177. [DOI], [ADS] (Cited on page 32.)
- McComas, D.J., Elliott, H.A., Schwadron, N.A., Gosling, J.T., Skoug, R.M. and Goldstein, B.E., 2003, “The three-dimensional solar wind around solar maximum”, *Geophys. Res. Lett.*, **30**, 1517. [DOI], [ADS] (Cited on page 11.)
- McComas, D.J., Velli, M., Lewis, W.S. et al., 2007, “Understanding coronal heating and solar wind acceleration: Case for in situ near-Sun measurements”, *Rev. Geophys.*, **45**, RG1004. [DOI], [ADS] (Cited on pages 6 and 11.)
- McComas, D.J., Ebert, R.W., Elliott, H.A., Goldstein, B.E., Gosling, J.T., Schwadron, N.A. and Skoug, R.M., 2008, “Weaker solar wind from the polar coronal holes and the whole Sun”, *Geophys. Res. Lett.*, **35**, L18103. [DOI], [ADS] (Cited on page 31.)
- McComas, D.J., Allegrini, F., Bochsler, P. et al., 2009, “IBEX–Interstellar Boundary Explorer”, *Space Sci. Rev.*, **146**, 11–33. [DOI], [ADS] (Cited on page 21.)
- McComas, D.J., Alexashov, D., Bzowski, M. et al., 2012, “The Heliosphere’s Interstellar Interaction: No Bow Shock”, *Science*, **336**, 1291–1293. [DOI], [ADS] (Cited on page 17.)
- McCracken, K.G., 2007, “Heliomagnetic field near Earth, 1428-2005”, *J. Geophys. Res.*, **112**, A09106. [DOI], [ADS] (Cited on page 35.)
- Mikić, Z., Linker, J.A., Schnack, D.D., Lionello, R. and Tarditi, A., 1999, “Magnetohydrodynamic modeling of the global solar corona”, *Phys. Plasmas*, **6**, 2217–2224. [DOI], [ADS] (Cited on page 7.)
- Moldwin, M.B., Ford, S., Lepping, R., Slavin, J. and Szabo, A., 2000, “Small-scale magnetic flux ropes in the solar wind”, *Geophys. Res. Lett.*, **27**, 57–60. [DOI], [ADS] (Cited on page 24.)
- Moses, D., 1987, “Jovian electrons at 1 AU: 1978–1984”, *Astrophys. J.*, **313**, 471–486. [DOI], [ADS] (Cited on page 20.)
- Mulligan, T., Russell, C.T. and Luhmann, J.G., 1998, “Solar cycle evolution of the structure of magnetic clouds in the inner heliosphere”, *Geophys. Res. Lett.*, **25**, 2959–2962. [DOI], [ADS] (Cited on page 25.)

- Murphy, N., Smith, E.J. and Schwadron, N.A., 2002, “Strongly underwound magnetic fields in co-rotating rarefaction regions: Observations and Implications”, *Geophys. Res. Lett.*, **29**(22), 2066. [DOI], [ADS] (Cited on page 22.)
- Mursula, K. and Hiltula, T., 2003, “Bashful ballerina: Southward shifted heliospheric current sheet”, *Geophys. Res. Lett.*, **30**, 2135. [DOI], [ADS] (Cited on page 23.)
- Muscheler, R., Joos, F., Beer, J., Müller, S.A., Vonmoos, M. and Snowball, I., 2007, “Solar activity during the last 1000 yr inferred from radionuclide records”, *Quat. Sci. Rev.*, **26**, 82–97. [DOI], [ADS] (Cited on page 35.)
- Nash, A.G., Sheeley Jr, N.R. and Wang, Y.-M., 1988, “Mechanisms for the rigid rotation of coronal holes”, *Solar Phys.*, **117**, 359–389. [DOI], [ADS] (Cited on pages 22 and 32.)
- Ness, N.F. and Wilcox, J.M., 1964, “Solar Origin of the Interplanetary Magnetic Field”, *Phys. Rev. Lett.*, **13**, 461–464. [DOI], [ADS] (Cited on page 9.)
- Neugebauer, M. and Goldstein, R., 1997, “Particle and field signatures of coronal mass ejections in the Solar Wind”, in *Coronal Mass Ejections*, (Eds.) Crooker, N.U., Joselyn, J.A., Feynman, J., Geophysical Monograph, 99, pp. 245–251, American Geophysical Union, Washington, DC. [DOI] (Cited on page 23.)
- Neugebauer, M., Goldstein, B.E., McComas, D.J., Suess, S.T. and Balogh, A., 1995, “Ulysses observations of microstreams in the solar wind from coronal holes”, *J. Geophys. Res.*, **100**(A12), 23,389–23,396. [DOI], [ADS] (Cited on page 26.)
- Neugebauer, M., Smith, E.J., Ruzmaikin, A., Feynman, J. and Vaughan, A.H., 2000, “The solar magnetic field and the solar wind: Existence of preferred longitudes”, *J. Geophys. Res.*, **105**, 2315–2324. [DOI], [ADS] (Cited on page 32.)
- Odstrčil, D., Pizzo, V.J., Linker, J.A., Riley, P., Lionello, R. and Mikić, Z., 2004, “Initial coupling of coronal and heliospheric numerical magnetohydrodynamic codes”, *J. Atmos. Sol.-Terr. Phys.*, **66**, 1311–1320. [DOI], [ADS] (Cited on page 14.)
- Owens, M.J., 2008, “Combining remote and in situ observations of coronal mass ejections to better constrain magnetic cloud reconstruction”, *J. Geophys. Res.*, **113**(A12), A12102. [DOI], [ADS] (Cited on pages 25 and 32.)
- Owens, M.J. and Crooker, N.U., 2006, “Coronal mass ejections and magnetic flux buildup in the heliosphere”, *J. Geophys. Res.*, **111**(A10), A10104. [DOI], [ADS] (Cited on pages 29 and 32.)
- Owens, M.J. and Crooker, N.U., 2007, “Reconciling the electron counterstreaming and dropout occurrence rates with the heliospheric flux budget”, *J. Geophys. Res.*, **112**, A06106. [DOI], [ADS] (Cited on pages 20 and 32.)
- Owens, M.J. and Lockwood, M., 2012, “Cyclic loss of open solar flux since 1868: The link to heliospheric current sheet tilt and implications for the Maunder Minimum”, *J. Geophys. Res.*, **117**, A04102. [DOI], [ADS] (Cited on pages 33 and 35.)
- Owens, M.J., Cargill, P.J., Pagel, C., Siscoe, G.L. and Crooker, N.U., 2005, “Characteristic magnetic field and speed properties of interplanetary coronal mass ejections and their sheath regions”, *J. Geophys. Res.*, **110**, A01105. [DOI], [ADS] (Cited on page 26.)
- Owens, M.J., Schwadron, N.A., Crooker, N.U., Hughes, W.J. and Spence, H.E., 2007, “Role of coronal mass ejections in the heliospheric Hale cycle”, *Geophys. Res. Lett.*, **34**, L06104. [DOI], [ADS] (Cited on page 32.)
- Owens, M.J., Arge, C.N., Crooker, N.U., Schwadron, N.A. and Horbury, T.S., 2008a, “Estimating total heliospheric magnetic flux from single-point in situ measurements”, *J. Geophys. Res.*, **113**(A12), A12103. [DOI], [ADS] (Cited on pages 25, 29, and 31.)

- Owens, M.J., Crooker, N.U. and Schwadron, N.A., 2008b, “Suprathermal electron evolution in a Parker spiral magnetic field”, *J. Geophys. Res.*, **113**(A12), A11104. [DOI], [ADS] (Cited on page 20.)
- Owens, M.J., Horbury, T.S. and Arge, C.N., 2010, “Probing the Large-scale Topology of the Heliospheric Magnetic Field using Jovian Electrons”, *Astrophys. J.*, **714**, 1617–1623. [DOI], [ADS] (Cited on page 20.)
- Owens, M.J., Crooker, N.U. and Lockwood, M., 2011a, “How is open solar magnetic flux lost over the solar cycle?”, *J. Geophys. Res.*, **116**, A04111. [DOI], [ADS] (Cited on pages 12 and 33.)
- Owens, M.J., Wicks, R.T. and Horbury, T.S., 2011b, “Magnetic Discontinuities in the Near-Earth Solar Wind: Evidence of In-Transit Turbulence or Remnants of Coronal Structure?”, *Solar Phys.*, **269**, 411–420. [DOI], [ADS] (Cited on pages 26 and 27.)
- Owens, M.J., Usoskin, I. and Lockwood, M., 2012, “Heliospheric modulation of galactic cosmic rays during grand solar minima: Past and future variations”, *Geophys. Res. Lett.*, **39**, L19102. [DOI], [ADS] (Cited on page 33.)
- Owens, M.J., Crooker, N.U. and Lockwood, M., 2013, “Solar origin of heliospheric magnetic field inversions: Evidence for coronal loop opening within pseudostreamers”, *J. Geophys. Res.*, **118**, 1868–1879. [DOI], [ADS] (Cited on page 23.)
- Pagel, C., Crooker, N.U., Larson, D.E., Kahler, S.W. and Owens, M.J., 2005, “Understanding electron heat flux signatures in the solar wind”, *J. Geophys. Res.*, **110**, A01103. [DOI], [ADS] (Cited on pages 20 and 32.)
- Pagel, C., Gary, S.P., de Koning, C.A., Skoug, R.M. and Steinberg, J.T., 2007, “Scattering of suprathermal electrons in the solar wind: ACE observations”, *J. Geophys. Res.*, **112**(A11), A04103. [DOI], [ADS] (Cited on page 20.)
- Parker, E.N., 1958, “Dynamics of the Interplanetary Gas and Magnetic Fields.”, *Astrophys. J.*, **128**, 664–676. [DOI], [ADS] (Cited on pages 5 and 8.)
- Phan, T.D., Gosling, J.T., Davis, M.S. et al., 2006, “A magnetic reconnection X-line extending more than 390 Earth radii in the solar wind”, *Nature*, **439**, 175–178. [DOI], [ADS] (Cited on page 26.)
- Pizzo, V.J., 1991, “The Evolution of Corotating Stream Fronts Near the Ecliptic Plane in the Inner Solar System. 2. Three-Dimensional Tilted-Dipole Fronts”, *J. Geophys. Res.*, **96**, 5405–5420. [DOI], [ADS] (Cited on pages 14 and 15.)
- Rees, A. and Forsyth, R.J., 2003, “Magnetic clouds with east/west orientated axes observed by Ulysses during solar cycle 23”, *Geophys. Res. Lett.*, **30**(19), 8030. [DOI], [ADS] (Cited on page 25.)
- Richardson, I.G., Cliver, E.W. and Cane, H.V., 2000, “Sources of geomagnetic activity over the solar cycle: Relative importance of coronal mass ejections, high-speed streams, and slow solar wind”, *J. Geophys. Res.*, **105**, 18,203–18,214. [DOI], [ADS] (Cited on pages 25 and 31.)
- Richardson, I.G., Cliver, E.W. and Cane, H.V., 2001, “Sources of geomagnetic storms for solar minimum and maximum conditions during 1972–2000”, *Geophys. Res. Lett.*, **28**, 2569–2572. [DOI], [ADS] (Cited on page 26.)
- Richardson, I.G., Cane, H.V. and Cliver, E.W., 2002, “Sources of geomagnetic activity during nearly three solar cycles (1972–2000)”, *J. Geophys. Res.*, **107**(A8), 1187. [DOI], [ADS] (Cited on pages 24 and 31.)
- Richardson, J.D. and Paularena, K.I., 1996, “Meridional flow in the solar wind”, *J. Geophys. Res.*, **101**, 19,995–20,002. [DOI], [ADS] (Cited on page 18.)
- Riley, P., Linker, J.A. and Mikić, Z., 2002, “Modeling the heliospheric current sheet: Solar cycle variations”, *J. Geophys. Res.*, **107**(A7), 1136. [DOI], [ADS] (Cited on page 28.)

- Riley, P., Gosling, J.T. and Crooker, N.U., 2004, “Ulysses Observations of the Magnetic Connectivity between Coronal Mass Ejections and the Sun”, *Astrophys. J.*, **608**, 1100–1105. [DOI], [ADS] (Cited on page 25.)
- Riley, P., Linker, J.A., Mikić, Z., Lionello, R., Ledvina, S.A. and Luhmann, J.G., 2006a, “A Comparison between Global Solar Magnetohydrodynamic and Potential Field Source Surface Model Results”, *Astrophys. J.*, **653**, 1510–1516. [DOI], [ADS] (Cited on page 7.)
- Riley, P., Schatzman, C., Cane, H.V., Richardson, I.G. and Gopalswamy, N., 2006b, “On the Rates of Coronal Mass Ejections: Remote Solar and In Situ Observations”, *Astrophys. J.*, **647**, 648–653. [DOI], [ADS] (Cited on pages 24 and 31.)
- Roelof, E.C., Simnett, G.M., Decker, R.B., Lanzerotti, L.J., MacLennan, C.G., Armstrong, T.P. and Gold, R.E., 1997, “Reappearance of recurrent low-energy particle events at Ulysses/HI-SCALE in the northern heliosphere”, *J. Geophys. Res.*, **102**, 11,251–11,262. [DOI], [ADS] (Cited on page 22.)
- Rosenbauer, H., Schwenn, R., Marsch, E. et al., 1977, “A survey on initial results of the HELIOS plasma experiment”, *J. Geophys.*, **42**(6), 561–580. [ADS] (Cited on page 19.)
- Rouillard, A.P., Sheeley Jr, N.R., Cooper, T.J. et al., 2011, “The Solar Origin of Small Interplanetary Transients”, *Astrophys. J.*, **734**, 7. [DOI], [ADS] (Cited on page 24.)
- Rust, D.M., 1994, “Spawning and shedding helical magnetic fields in the solar atmosphere”, *Geophys. Res. Lett.*, **21**, 241–244. [DOI], [ADS] (Cited on page 25.)
- Savani, N.P., Owens, M.J., Rouillard, A.P. et al., 2011, “Evolution of Coronal Mass Ejection Morphology with Increasing Heliocentric Distance. II. In Situ Observations”, *Astrophys. J.*, **732**, 117. [DOI], [ADS] (Cited on page 26.)
- Scearce, C., Cantarano, S., Ness, N., Mariani, F., Terenzi, R. and Burlaga, L., 1975, “The Rome-GSFC magnetic field experiment for Helios A and B (E3)”, *Raumfahrtforschung*, **19**, 237–240. [ADS] (Cited on page 5.)
- Schatten, K.H., 1971, “Current sheet magnetic model for the solar corona”, *Cosmic Electrodyn.*, **2**, 232–245. [ADS] (Cited on page 7.)
- Schatten, K.H., Wilcox, J.M. and Ness, N.F., 1969, “A model of interplanetary and coronal magnetic fields”, *Solar Phys.*, **6**, 442–455. [DOI], [ADS] (Cited on pages 7 and 8.)
- Schrijver, C.J. and DeRosa, M.L., 2003, “Photospheric and heliospheric magnetic fields”, *Solar Phys.*, **212**, 165–200. [DOI], [ADS] (Cited on page 31.)
- Schulz, M., 1973, “Interplanetary sector structure and the heliomagnetic equator”, *Astrophys. Space Sci.*, **24**, 371–383. [DOI], [ADS] (Cited on page 10.)
- Schwadron, N.A., 2002, “An explanation for strongly underwound magnetic field in co-rotating rarefaction regions and its relationship to footpoint motion on the the sun”, *Geophys. Res. Lett.*, **29**, 1663. [DOI], [ADS] (Cited on page 22.)
- Schwadron, N.A. and McComas, D.J., 2003, “Solar Wind Scaling Law”, *Astrophys. J.*, **599**, 1395–1403. [DOI], [ADS] (Cited on page 26.)
- Schwadron, N.A., Fisk, L.A. and Zurbuchen, T.H., 1999, “Elemental Fractionation in the Slow Solar Wind”, *Astrophys. J.*, **521**, 859–867. [DOI], [ADS] (Cited on page 32.)
- Schwadron, N.A., McComas, D.J. and DeForest, C., 2006, “Relationship between Solar Wind and Coronal Heating: Scaling Laws from Solar X-Rays”, *Astrophys. J.*, **642**, 1173–1176. [DOI], [ADS] (Cited on page 26.)



- Schwadron, N.A., Allegrini, F., Bzowski, M. et al., 2011, “Separation of the Interstellar Boundary Explorer Ribbon from Globally Distributed Energetic Neutral Atom Flux”, *Astrophys. J.*, **731**, 56. [DOI], [ADS] (Cited on page 17.)
- Schwenn, R., 2006, “Space Weather: The Solar Perspective”, *Living Rev. Solar Phys.*, **3**, lrsp-2006-2. [DOI], [ADS]. URL (accessed 17 April 2013): <http://www.livingreviews.org/lrsp-2006-2> (Cited on page 23.)
- Shiota, D., Tsuneta, S., Shimojo, M., Sako, N., Orozco Suárez, D. and Ishikawa, R., 2012, “Polar Field Reversal Observations with Hinode”, *Astrophys. J.*, **753**, 157. [DOI], [ADS], [arXiv:1205.2154 [astro-ph.SR]] (Cited on page 31.)
- Shodhan, S., Crooker, N.U., Kahler, S.W., Fitzenreiter, R.J., Larson, D.E., Lepping, R.P., Siscoe, G.L. and Gosling, J.T., 2000, “Counterstreaming electrons in magnetic clouds”, *J. Geophys. Res.*, **105**, 27,261–27,268. [DOI], [ADS] (Cited on page 25.)
- Simpson, J.A., Zhang, M. and Bame, S., 1996, “A Solar Polar North-South Asymmetry for Cosmic-Ray Propagation in the Heliosphere: The Ulysses Pole-to-Pole Rapid Transit”, *Astrophys. J. Lett.*, **465**, L69–L72. [DOI], [ADS] (Cited on page 23.)
- Siscoe, G. and Odstrčil, D., 2008, “Ways in which ICME sheaths differ from magnetosheaths”, *J. Geophys. Res.*, **113**(A12), A00B07. [DOI], [ADS] (Cited on page 26.)
- Slavin, J.A. and Smith, E.J., 1983, “Solar cycle variations in the interplanetary magnetic field”, in *Solar Wind Five*, Proceedings of a conference held in Woodstock, Vermont, November 1–5 1982, (Ed.) Neugebauer, M., NASA Conference Publication, 2280, pp. 323–331, NASA, Washington, DC. [ADS] (Cited on page 31.)
- Smith, E.J., 1990, “The heliospheric current sheet and modulation of Galactic cosmic rays”, *J. Geophys. Res.*, **95**, 18,731–18,743. [DOI], [ADS] (Cited on page 20.)
- Smith, E.J., 2008, “The global heliospheric magnetic field”, in *The Heliosphere through the Solar Activity Cycle*, (Eds.) Balogh, A., Lanzerotti, L.J., Suess, S.T., Springer–Praxis Books in Astronomy and Space Sciences, chap. 4, pp. 79–150, Springer; Praxis, Berlin; New York; Chichester. [DOI], [ADS] (Cited on pages 5 and 23.)
- Smith, E.J. and Balogh, A., 1995, “Ulysses observations of the radial magnetic field”, *Geophys. Res. Lett.*, **22**, 3317–3320. [DOI], [ADS] (Cited on page 10.)
- Smith, E.J. and Balogh, A., 2003, “Open Magnetic Flux: Variation with Latitude and Solar Cycle”, in *Solar Wind Ten*, Proceedings of the Tenth International Solar Wind Conference, Pisa, Italy, 17–21 June 2002, (Eds.) Velli, M., Bruno, R., Malara, F., AIP Conference Proceedings, 679, pp. 67–70, American Institute of Physics, Melville, NY. [DOI], [ADS] (Cited on pages 10, 29, and 31.)
- Smith, E.J. and Balogh, A., 2008, “Decrease in heliospheric magnetic flux in this solar minimum: Recent Ulysses magnetic field observations”, *Geophys. Res. Lett.*, **35**, L22103. [DOI], [ADS] (Cited on page 31.)
- Smith, E.J. and Wolfe, J.H., 1976, “Observations of interaction regions and corotating shocks between one and five AU: Pioneers 10 and 11”, *Geophys. Res. Lett.*, **3**, 137–140. [DOI], [ADS] (Cited on pages 14 and 15.)
- Smith, E.J., Connor, B.V. and Foster Jr, G.T., 1975, “Measuring the Magnetic Fields of Jupiter and the Outer Solar System”, *IEEE Trans. Magn.*, **11**, 962–980. [DOI], [ADS] (Cited on page 5.)
- Smith, E.J., Balogh, A., Neugebauer, M. and McComas, D., 1995, “Ulysses observations of Alfvén waves in the southern and northern solar hemispheres”, *Geophys. Res. Lett.*, **22**, 3381–3384. [DOI], [ADS] (Cited on page 26.)

- Smith, E.J., Jokipii, J.R., Kóta, J., Lepping, R.P. and Szabo, A., 2000, “Evidence of a North-South Asymmetry in the Heliosphere Associated with a Southward Displacement of the Heliospheric Current Sheet”, *Astrophys. J.*, **533**, 1084–1089. [DOI], [ADS] (Cited on page 23.)
- Solanki, S.K., Schüssler, M. and Fligge, M., 2000, “Evolution of the Sun’s large-scale magnetic field since the Maunder minimum”, *Nature*, **408**, 445–447. [DOI], [ADS] (Cited on page 33.)
- Solanki, S.K., Usoskin, I.G., Kromer, B., Schüssler, M. and Beer, J., 2004, “Unusual activity of the Sun during recent decades compared to the previous 11,000 years”, *Nature*, **431**, 1084–1087. [DOI], [ADS] (Cited on page 35.)
- St Cyr, O.C., Howard, R.A., Sheeley Jr, N.R. et al., 2000, “Properties of coronal mass ejections: SOHO LASCO observations from January 1996 to June 1998”, *J. Geophys. Res.*, **105**, 18,169–18,186. [DOI], [ADS] (Cited on pages 28, 29, and 32.)
- Steinberg, J.T., Gosling, J.T., Skoug, R.M. and Wiens, R.C., 2005, “Suprathermal electrons in high-speed streams from coronal holes: Counterstreaming on open field lines at 1 AU”, *J. Geophys. Res.*, **110**(A9), A06103. [DOI], [ADS] (Cited on page 20.)
- Steinhilber, F., Abreu, J.A., Beer, J. and McCracken, K.G., 2010, “Interplanetary magnetic field during the past 9300 years inferred from cosmogenic radionuclides”, *J. Geophys. Res.*, **115**, A01104. [DOI], [ADS] (Cited on page 35.)
- Stone, E.C., Cummings, A.C., McDonald, F.B., Heikkila, B.C., Lal, N. and Webber, W.R., 2005, “Voyager 1 Explores the Termination Shock Region and the Heliosheath Beyond”, *Science*, **309**, 2017–2020. [DOI], [ADS] (Cited on page 17.)
- Stone, E.C., Cummings, A.C., McDonald, F.B., Heikkila, B.C., Lal, N. and Webber, W.R., 2008, “An asymmetric solar wind termination shock”, *Nature*, **454**, 71–74. [DOI], [ADS] (Cited on page 17.)
- Suess, S.T. and Smith, E.J., 1996, “Latitudinal dependence of the radial IMF component: Coronal imprint”, *Geophys. Res. Lett.*, **23**, 3267–3270. [DOI], [ADS] (Cited on page 10.)
- Svalgaard, L., 1972, “Interplanetary Magnetic-Sector Structure, 1926–1971”, *J. Geophys. Res.*, **77**, 4027–4034. [DOI], [ADS] (Cited on page 33.)
- Svalgaard, L. and Cliver, E.W., 2005, “The *IDV* index: Its derivation and use in inferring long-term variations of the interplanetary magnetic field strength”, *J. Geophys. Res.*, **110**(A9), A12103. [DOI], [ADS] (Cited on page 33.)
- Svalgaard, L. and Cliver, E.W., 2010, “Heliospheric magnetic field 1835–2009”, *J. Geophys. Res.*, **115**, A09111. [DOI], [ADS], [arXiv:1002.2934] (Cited on pages 33 and 34.)
- Svalgaard, L. and Wilcox, J.M., 1975, “Long-term evolution of solar sector structure”, *Solar Phys.*, **41**, 461–475. [DOI], [ADS] (Cited on page 14.)
- Svalgaard, L., Cliver, E.W. and Kamide, Y., 2005, “Sunspot cycle 24: Smallest cycle in 100 years?”, *Geophys. Res. Lett.*, **32**, L01104. [DOI], [ADS] (Cited on page 31.)
- Teegarden, B.J., McDonald, F.B., Trainor, J.H., Webber, W.R. and Roelof, E.C., 1974, “Interplanetary MeV electrons of Jovian origin”, *J. Geophys. Res.*, **79**, 3615–3622. [DOI], [ADS] (Cited on page 20.)
- Thomas, B.T. and Smith, E.J., 1980, “The Parker spiral configuration of the interplanetary magnetic field between 1 and 8.5 AU”, *J. Geophys. Res.*, **85**, 6861–6867. [DOI], [ADS] (Cited on page 10.)
- Thomas, B.T. and Smith, E.J., 1981, “The structure and dynamics of the heliospheric current sheet”, *J. Geophys. Res.*, **86**, 11,105–11,110. [DOI], [ADS] (Cited on page 15.)

- Thomas, B.T., Slavin, J.A. and Smith, E.J., 1986, “Radial and Latitudinal Gradients in the Interplanetary Magnetic Field: Evidence for Meridional Flux Transport”, *J. Geophys. Res.*, **91**, 6760–6764. [DOI], [ADS] (Cited on page 17.)
- Thomas, S.R., Owens, M.J. and Lockwood, M., 2013, “The 22-Year Hale Cycle in Cosmic Ray Flux – Evidence for Direct Heliospheric Modulation”, *Solar Phys.*, **289**, 407–421. [DOI], [ADS], [arXiv:1304.5191 [astro-ph.SR]] (Cited on page 20.)
- Tóth, G., Sokolov, I.V., Gombosi, T.I. et al., 2005, “Space Weather Modeling Framework: A new tool for the space science community”, *J. Geophys. Res.*, **110**(A9), A12226. [DOI], [ADS] (Cited on page 7.)
- Tsurutani, B.T., Gonzalez, W.D., Tang, F., Akasofu, S.I. and Smith, E.J., 1988, “Origin of Interplanetary Southward Magnetic Fields Responsible for Major Magnetic Storms Near Solar Maximum (1978–1979)”, *J. Geophys. Res.*, **93**, 8519–8531. [DOI], [ADS] (Cited on page 26.)
- Tu, C.-Y. and Marsch, E., 1993, “A model of solar wind fluctuations with two components: Alfvén waves and convective structures”, *J. Geophys. Res.*, **98**(17), 1257–1276. [DOI], [ADS] (Cited on page 26.)
- Tu, C.-Y. and Marsch, E., 1995, “MHD structures, waves and turbulence in the solar wind: Observations and theories”, *Space Sci. Rev.*, **73**(1/2), 1–210. [DOI], [ADS] (Cited on page 26.)
- Usoskin, I.G., 2013, “A History of Solar Activity over Millennia”, *Living Rev. Solar Phys.*, **10**, lrsp-2013-1. [DOI], [ADS]. URL (accessed 7 November 2013): <http://www.livingreviews.org/lrsp-2013-1> (Cited on pages 20 and 35.)
- Usoskin, I.G., Alanko-Huotari, K., Kovaltsov, G.A. and Mursula, K., 2005, “Heliospheric modulation of cosmic rays: Monthly reconstruction for 1951–2004”, *J. Geophys. Res.*, **110**(A9), A12108. [DOI], [ADS] (Cited on page 35.)
- Verdini, A. and Velli, M., 2007, “Alfvén Waves and Turbulence in the Solar Atmosphere and Solar Wind”, *Astrophys. J.*, **662**, 669–676. [DOI], [ADS], [astro-ph/0702205] (Cited on page 26.)
- Vieira, L.E.A. and Solanki, S.K., 2010, “Evolution of the solar magnetic flux on time scales of years to millenia”, *Astron. Astrophys.*, **509**, A100. [DOI], [ADS], [arXiv:0911.4396 [astro-ph.SR]] (Cited on page 33.)
- Wang, Y.-M. and Sheeley Jr, N.R., 1990, “Solar wind speed and coronal flux-tube expansion”, *Astrophys. J.*, **355**, 726–732. [DOI], [ADS] (Cited on pages 10 and 11.)
- Wang, Y.-M. and Sheeley Jr, N.R., 1995, “Solar Implications of Ulysses Interplanetary Field Measurements”, *Astrophys. J. Lett.*, **447**, L143–L146. [DOI], [ADS] (Cited on page 7.)
- Wang, Y.-M. and Sheeley Jr, N.R., 2003, “On the Topological Evolution of the Coronal Magnetic Field During the Solar Cycle”, *Astrophys. J.*, **599**, 1404–1417. [DOI], [ADS] (Cited on pages 6, 31, and 32.)
- Wang, Y.-M. and Sheeley Jr, N.R., 2004, “Footpoint Switching and the Evolution of Coronal Holes”, *Astrophys. J.*, **612**, 1196–1205. [DOI], [ADS] (Cited on pages 22 and 32.)
- Wang, Y.-M., Hawley, S.H. and Sheeley Jr, N.R., 1996, “The Magnetic Nature of Coronal Holes”, *Science*, **271**, 464–469. [DOI], [ADS] (Cited on page 7.)
- Wang, Y.-M., Lean, J. and Sheeley Jr, N.R., 2000a, “The long-term variation of the Sun’s open magnetic flux”, *Geophys. Res. Lett.*, **27**, 505–508. [DOI], [ADS] (Cited on pages 29 and 32.)
- Wang, Y.-M., Sheeley Jr, N.R. and Lean, J., 2000b, “Understanding the evolution of the Sun’s open magnetic flux”, *Geophys. Res. Lett.*, **27**, 621–624. [DOI], [ADS] (Cited on page 29.)
- Wang, Y.-M., Robbrecht, E. and Sheeley Jr, N.R., 2009, “On the Weakening of the Polar Magnetic Fields during Solar Cycle 23”, *Astrophys. J.*, **707**, 1372–1386. [DOI], [ADS] (Cited on page 31.)

- Webb, D.F. and Howard, R.A., 1994, “The solar cycle variation of coronal mass ejections and the solar wind mass flux”, *J. Geophys. Res.*, **99**, 4201–4220. [DOI], [ADS] (Cited on pages 25 and 33.)
- Webber, W.R. and Lockwood, J.A., 1988, “Characteristics of the 22-year modulation of cosmic rays as seen by neutron monitors”, *J. Geophys. Res.*, **93**, 8735–8740. [DOI], [ADS] (Cited on page 20.)
- Wenzel, K.-P., Marsden, R.G., Page, D.E. and Smith, E.J., 1992, “The ULYSSES Mission”, *Astron. Astrophys. Suppl.*, **92**, 207–219. [ADS] (Cited on page 10.)
- Wilcox, J.M. and Ness, N.F., 1965, “Quasi-Stationary Corotating Structure in the Interplanetary Medium”, *J. Geophys. Res.*, **70**(23), 5793–5805. [DOI], [ADS] (Cited on pages 9 and 11.)
- Wimmer-Schweingruber, R.F., Crooker, N.U., Balogh, A. et al., 2006, “Understanding Interplanetary Coronal Mass Ejection Signatures. Report of Working Group B”, *Space Sci. Rev.*, **123**, 177–216. [DOI], [ADS] (Cited on page 23.)
- Winterhalter, D., Smith, E.J., Slavin, J.A. and Wolfe, J.H., 1990, “Spatial gradients in the heliospheric magnetic field: Pioneer 11 observations between 1 AU and 24 AU, and over solar cycle 21”, *J. Geophys. Res.*, **95**, 1–11. [DOI], [ADS] (Cited on pages 17 and 18.)
- Woo, R., 2005, “Relating White-Light Coronal Images to Magnetic Fields and Plasma Flow”, *Solar Phys.*, **231**, 71–85. [DOI], [ADS] (Cited on page 7.)
- Yashiro, S., Gopalswamy, N., Michalek, G., St Cyr, O.C., Plunkett, S.P., Rich, N.B. and Howard, R.A., 2004, “A catalog of white light coronal mass ejections observed by the SOHO spacecraft”, *J. Geophys. Res.*, **109**, A07105. [DOI], [ADS] (Cited on pages 29 and 32.)
- Yeates, A.R., Mackay, D.H., van Ballegoijen, A.A. and Constable, J.A., 2010, “A nonpotential model for the Sun’s open magnetic flux”, *J. Geophys. Res.*, **115**, A09112. [DOI], [ADS], [arXiv:1006.4011 [astro-ph.SR]] (Cited on page 32.)
- Zank, G.P., 1999, “Interaction of the solar wind with the local interstellar medium: a theoretical perspective”, *Space Sci. Rev.*, **89**, 413–688. [DOI], [ADS] (Cited on page 17.)
- Zhao, X. and Hoeksema, J.T., 1996, “Effect of coronal mass ejections on the structure of the heliospheric current sheet”, *J. Geophys. Res.*, **101**, 4825–4834. [DOI], [ADS] (Cited on page 25.)
- Zhou, X. and Smith, E.J., 2009, “Solar cycle variations of heliospheric magnetic flux”, *J. Geophys. Res.*, **114**, A03106. [DOI], [ADS] (Cited on page 31.)
- Zurbuchen, T.H., 2007, “A New View of the Coupling of the Sun and the Heliosphere”, *Annu. Rev. Astron. Astrophys.*, **45**, 297–338. [DOI], [ADS] (Cited on page 5.)
- Zurbuchen, T.H., Schwadron, N.A. and Fisk, L.A., 1997, “Direct observational evidence for a heliospheric magnetic field with large excursions in latitude”, *J. Geophys. Res.*, **102**, 24,175–24,181. [DOI], [ADS] (Cited on page 22.)
- Zurbuchen, T.H., Fisk, L.A., Gloeckler, G. and Schwadron, N.A., 1998, “Element and Isotopic Fractionation in Closed Magnetic Structures”, *Space Sci. Rev.*, **85**, 397–406. [DOI], [ADS] (Cited on page 32.)